FLOOR SENSOR DEVELOPMENT USING SIGNAL SCAVENGING FOR PERSONNEL DETECTION SYSTEM

A Thesis

Presented to

The Faculty of the Graduate School

At the University of Missouri-Columbia

In Partial Fulfillment

Of the Requirements for the Degree

Master of Science

---

by

ROHAN VASANTHA NEELGUND

Dr. Harry Tyrer, Thesis Supervisor

JULY 2010

The undersigned, appointed by the dean of the Graduate School, have examined the thesis entitled

FLOOR SENSOR DEVELOPMENT USING SIGNAL SCAVENGING FOR PERSONNEL DETECTION SYSTEM

Presented by

Rohan Vasantha Neelgund,

A candidate for the degree of

Master of Science

And hereby certify that, in their opinion, it is worthy of acceptance.

Dr. Harry Tyrer

Dr. Marjorie Skubic

Dr. John Fresen

ACKNOWLEDGEMENTS

I would like to take this opportunity to thank Dr. Harry Tyrer who has guided me through the completion of my graduate studies in University of Missouri. I would like to thank him for the enormous patience he has shown with me throughout the course of my graduate studies. Of the many valuable things I have learned from him, the most important are patience and persistence, which I intend to apply in my everyday life. I would like to sincerely thank the members of my thesis committee; Dr. John Fresen and Dr. Marjorie Skubic for giving very valuable reviews regarding my thesis and regarding the presentation of my research.

I would like to thank all my colleagues who have helped me throughout my graduate studies. I would like to first thank all my project partners Uday Shriniwar, KrishnaKishor Devarakonda for consistently helping me and boosting me in my work. I would also like to thank Karthik Peddi, Srinivasan D for their extreme support in manufacturing the carpet. I would also like to thank Amit Dhatrak for his extended help with MS Excel.

Last but by no means the least; I whole-heartedly thank Richard Oberto for his great help, advices and laboratory instruments utilized to make this project successful. I sincerely thank my family and friends back in India whose constant support and faith helped me successfully complete my graduate studies in the United States. I would also like to thank Alzheimer's Association for funding our project under the ETAC program.

TABLE OF CONTENTS

LIST OF FIGURES

LIST OF TABLES

ABSTRACT

Falls have been a major cause of injuries likes fractures, head trauma in elder people. In many cases, these injuries have been fatal. This being a major concern of the Alzheimer's Association, a 'Smart Carpet' to detect a person's fall and accordingly generate an alarm was important. We developed faux floors and an actual floor for testing and demonstration to detect motion. We used a novel technique of signal scavenging to detect presence of the person. Aluminum foils were used as sensors as they were conducive to the applied pressure on them. Rigorous tests and experiments were performed on the faux floor sized 1m x 1m (3feet x 3feet) and 2.1m x 1m (7feet x 3feet) using these aluminum sensors. The noisy output pattern of the aluminum sensor was signal conditioned and converted into digital format using Op-Amps. The digital signal was later interfaced with a micro-controller unit and displayed onto a PC. Graphical analysis with ROC space and personal experience with utilization of the faux floor system gave us confidence to develop a real floor of the size 3.6m x 3.6m (12feet x 12feet). The results obtained on the full floor were beyond the expectations. Previously observed problems like cross-talk, noise interference and abrupt output behavior of the sensor system were avoided with careful manufacturing of carpet and earthing. With the development of the full floor, we have created a prototype which has high reliability and accuracy to detect motion and can be extensively used for further research.

CHAPTER 1 : INTRODUCTION

1.1. Motivation

Many gait observation and fall detection techniques have been developed by researchers using various techniques. Fall detection techniques have found profound applications among elderly patients who suffer from Alzheimer's disease. We intended to develop such a system which would detect person walking and possibly monitor falls. Building such a system would improve independence among the elderly Alzheimer's patients who suffer from forgetfulness, challenges in planning, difficulty completing familiar tasks at home, poor judgment of tasks and so on (1). Providing internet connectivity to a monitoring system helps caregivers and distantly located family members to know the status about their loved ones by logging onto a website. The 'Smart Carpet' we developed is a cheap and reliable system which can consistently detect personnel walking and can be possibly used to detect falls on it.

1.2. Approach

We used aluminum foils as sensors to detect the presence of a person. Faux floor carpets using aluminum foils as sensors were developed to test its performance. Two faux floors and one real floor were built underneath which these aluminum foils were installed. The signals generated from the aluminum foil are a result of signal scavenging technique (4). These signals, which are 60Hz noise and its odd harmonics, are then fed through a three stage non-linear analog circuit. This circuit performs the signal conditioning on the input wave and is then passed into a microprocessor and finally into a computer. The

analog signal conditioning unit developed is a simple and low cost solution to detect the 60Hz noisy pattern from the aluminum foil sensor (A.2).

1.3. Outcome

We have successfully built and tested faux floors and an installed carpet using aluminum foil sensors. These floors have produced satisfactory results in terms of efficiency, accuracy and repeatability. We have published initial results of the one of the faux floor (development faux floor) that we created (16). The developed system with further improvements would definitely suffice the needs of a monitoring system for elderly patients with Alzheimer's disease. This dissertation focuses on the evolution of the analog circuitry which passively detects the footsteps of personnel walking on the carpet.

CHAPTER 2 : LITERATURE REVIEW

Studies indicate that older adults were concerned about falls and that they perceived technologies that monitor activity levels as useful. The major injuries observed were fractures and head trauma. It has been found that patients suffering from Alzheimer's disease have a symptom to fall even during their normal gait. The literature shows that seniors with cognitive impairment fall at an annual rate of 60% (1) i.e. almost one in two cognitively impaired person falls which is dangerous. Also, it is found that falls form the second leading cause of death for elders 79 years and older (2). It was found in elderly people that one in ten falls left the faller unable to get up for at least 5 minutes (3). Moreover, it is observed that it becomes very difficult for an aged person to recover from any type of injuries. Also, during old age, doctors restrict the usage of high dosage of several antibiotics depending on the patient's medical history.

Common symptoms of Alzheimer's disease are forgetfulness, challenges in planning, difficulty completing familiar tasks at home, poor judgment of tasks and so on. Since patients suffering from Alzheimer's disease have cognitive disabilities, they have an increased risk of falls over the general population. Consequently, flooring with the potential to detect falls is essential.

We intended to detect the presence of a person on a carpet using signal scavenging technique. This dissertation discusses the performance of the sensors used for signal scavenging; the development of faux floors for testing the performances, and the design and development of analog electronics required to signal condition these signal scavenging sensors.

The study focused on the of use signal scavenging as a means to monitor the elderly for motion and falls. Many unobtrusive applications to monitor the elderly have been developed (4). Unobtrusive means the individual has given their explicit permission for this monitoring and aware of it, the individual need take no action to effect the operation or performance of the system and the individual's privacy is not violated. There have been systems which determine the gait of a person. An algorithm for 'Smart Carpet' to sense the gait of a person was developed by sensor networks that identified the footsteps and footstep patterns (5). In a Semi-Markov based footstep pattern matching model, Electro-Mechanical Film was used as a thin, flexible, low-priced electret material to detect and study the motion of personnel (6). A reconfigurable high resolution floor using pressure sensitive polymer between conductive traces on Mylar sheet was also developed to study the human dance movements. However, this floor incorporated 6mm x 6mm sized 4,032 sensors covering an area of about 4160 square centimeters (7).

Many approaches to detect falls have been developed, with the use of accelerometer, floor vibrations (2), video cameras (8) (9); infra-red sensors (10), acoustic sensors (11). Radio Frequency Identification (RFID) tags were attached to the upper body (wrists) and to lower body (socks) to detect falls of a person (12). Most of the sensors used in the above techniques are either obsolete (no more into production) [accelerometer MMA7261Q, manufactured by Freescale Semiconductor, ADXL202, 2-axis accelerometer sensor manufactured by Analog Devices] or too expensive [NI USB-6210 price $250] to be used in manufacturing of carpet envisioned (13). Many of these systems require a stationery computer for the data from the sensors to be collected and gathered (11). The forgetfulness of Alzheimer's patients limits the use of wearable sensors. They

forget to wear the device so they need a monitoring system. The carpet we built is such a system. A cheap and highly efficient fall detection system was developed at the University of Virginia which incorporated the use of piezo transducers. The piezo sensor was placed in a special kit that required specialized signal processing algorithm. The inherently radial nature of the sensor made it sensitive (2).

Signal scavenging is analogous to energy scavenging: seemingly ubiquitous small energy in the environs provide the signal for use as a personnel sensor. Such energy which consists of 60Hz of noise and other stray electromagnetic field can be used to detect motion, and possibly falls. We propose using this noise pattern as an inherent source of signal generation (4). Stray signals were detected in aluminum foil as voltage differences between touched foil (say by hand) compared to that untouched. In particular we utilized the fact that the noise level read from a sample of aluminum foil increased when touched by a person. The signal characteristics of the aluminum foil contained 60Hz and its odd harmonics which is equivalent to the random noise present in atmosphere. The noise amplitude changes upon activation due to the antenna effect. Similar to the antenna, the aluminum foil produces a change in electric voltage corresponding to the change in the nearby electromagnetic field. This change in the electromagnetic waves is analogous to the ripples caused by throwing a stone in a pond producing crests and troughs. The use of aluminum foil to detect pressure was not an obvious choice. Sets of experiments using flexible organic field effect transistors were performed; these sensors are under development at the University of Cagliari and not ready for use (14). We turned to aluminum foils as an alternative that served us well.

Searching the internet for signal scavenging produces limited results. But, capacitive sensing used to detect the proximity, motion on the basis of capacitive coupling is better known (18). The performance of the capacitive sensors is found to be dependent on their shape and size. Additionally, the distance between the sensors and the inclusion of a ground plane to reduce the stray capacitances and interferences due to cross talk has been decisive for the design of the sensors. The use of capacitive sensing also depends on the environment in which the sensor is installed. Sensors possibly cannot be used in high radio and static- charged field where the possibility of the stray electromagnetic fields affecting the performance is more. The application of capacitances to detect touch has been implemented in numerous touch sensing applications (example: Iphone). Our technique uses antenna effects to detect the presence and hence the motion of person using the most commonly available capacitive sensors, aluminum foils (19).

CHAPTER 3 : METHODS

This chapter is divided into three parts. The first part consists of the faux floor design and construction, followed by the design and construction of the electronics unit. Later on, the performance testing of the faux floors is also discussed and directed to the results chapter.

4.1. Faux Floor Construction

We built two designs of the faux floor, 2x2 and 7x3 which were constructed on a faux wood floor. A real floor of the size 2.4m x 1.2m (8feet x 4feet) was also built after the successful testing of the development and prototype boards. The construction of each of these floors is described below.

4.1.1. Development System: A 2x2 Sensor Faux Floor:

We constructed a faux floor by placing a 1m x 1m x 16 mm (3 ft sq ¾ inches) thick piece of ply-wood board on a square frame of 5 cm x 10 cm (2" X 4") wood studs and is termed as Development Floor. A suitable stud provided additional support at the center. The development floor, also called as 2x2 faux floor consisted of four sensors arranged in a two-dimensional matrix format. An institutional carpet of the same size as that of the wooden frame covered these sensors.

3.1.1.1. Sensor layers and layout:

The sensor layout contained two layers of aluminum foils and plastic sheet respectively. The arrangement of these aluminum foils and plastic sheet was equivalent to a capacitor design, having a positive and a ground plate and a dielectric medium between the two (see Figure 3.1). The aluminum sensors had the plastic sheet acting as dielectric medium. A rectangular shaped aluminum foil was placed at the bottom of the layout and we termed as it as the sensor layer. The size of rectangle varied with the sensor floor design. A multi-strand wire was soldered to one corner of this rectangular foil. A plastic sheet of the carpet size acting as a dielectric medium was placed in between the aluminum sensors and the ground plane. An aluminum foil floor termed as ground plane was placed above the dielectric plastic sheet and was connected to the earth/system ground. The ground plane prevented both, the stray parasitic capacitance and presence of a conductive object, which are related to the electric-field's path to ground.

The ground plane was of the same size as that of the carpet. This ground layer was again followed by a layer of plastic sheet to protect the aluminum ground plane from wear and tear that may be caused during shifting of the carpet. The top of the faux floor was marked as A, B, C, and D to indicate the four sensors underneath the floor (see Figure 3.2).

Figure 3.1: Arrangement of the 2x2 Development System layers. Plastic sheet covered the wooden base followed by ground plane, plastic sheet and finally the sensor layer.

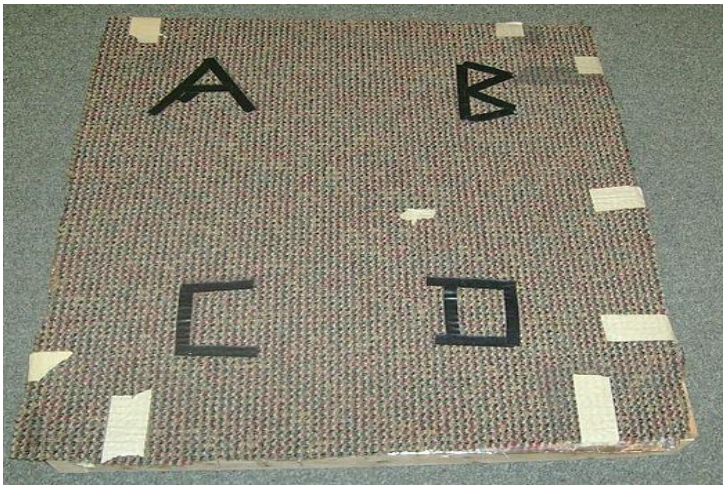

Figure 3.2: Development floor consisting of a wooden faux floor covered with a carpet. The size of the board is 1m x 1m. The sensors are laid in between the carpet and the wooden floor. The wooden base consists of a wooden frame onto which a ply board is fixed with studs. A, B, C and D indicate the four sensors lay below the carpet.

4.1.2. Prototype System: A 7x3 Sensor Faux Floor:

The size of this faux floor was 2.1m x 1m (7feet x 3feet) and we termed this floor as the prototype system. The prototype system also called as 7x3 faux floor consisted of twenty-one sensors arranged in seven rows and three columns matrix format. A 2.1m x 1m sized wooden frame was kept beneath the sensor floor. A carpet of same size as that of the wooden frame covered these sensors.

3.1.1.2. Sensor Layers and Layout

The arrangement of the sensors for the prototype system was similar to the layout in Figure 3.4. A wooden base of the size 2.13m x 0.91m was placed under the sensors. The top of the sensor was covered with a carpet same size as that of the wooden base. The sensors were arranged in a 7x3 matrix format. All the wires from one column were

grouped together and crimped into a header connector. Thus, the prototype system had three header connectors; each representing one column. The top of the faux floor (carpet) was marked as A1 to A7, B1 to B7 and C1 to C7 to indicate the numbering of the sensors below as shown in Figure 3.3.

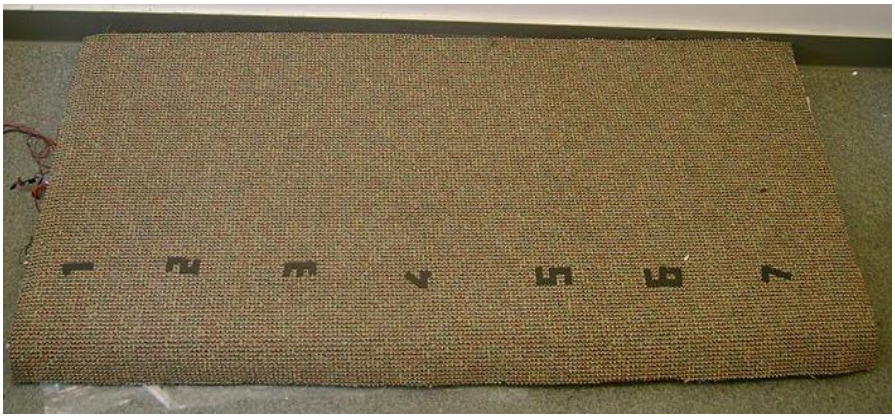

Figure 3.3: Prototype floor consisting of a wooden faux floor covered with a carpet. The size of the floor is 2.1m x 1m and consists of 21 sensors. The sensors are laid in between the carpet and the wooden floor. The wooden base consists of a wooden frame onto which a ply-board is fixed with studs. The numbering on the carpet indicates the sensor number below the carpet.

4.2. Installed Floor: A sensor floor containing 132 sensors placed 15.2cms apart.

This floor was aimed to create a floor to occupy a room of the size 3.6m x 3.6m (12feet x 12feet). An installation segment of the size 2.4m x 1.2m (8feet x 4feet) was developed and had a similar design as mentioned in Figure 3.1. This segment and the floor were placed on a carpet instead of a wooden base.

4.2.1. Sensor Layout:

The installation segment had 32 sensors arranged in 8 rows and 4 columns matrix format. The size of installation segment was 2.4m x 1.2m. Four such installation

segments were made thus accounting to 128 sensors. The size of the sensors was 15.2cm x 15.2cm (6in x 6in) and the spacing between adjacent sensors was 30.5cm (1foot). Figure 3.4 is a pictorial arrangement of the sensor layout which is followed for the installed carpet.

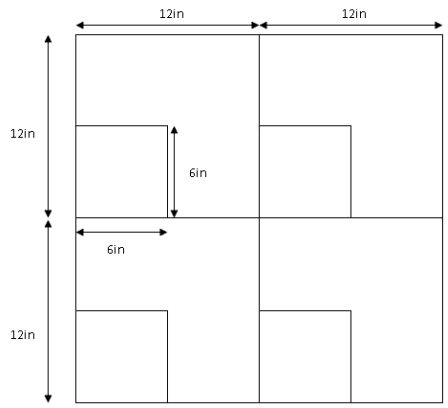

Figure 3.4: Sample pictorial arrangement of the sensor foil on the plastic sheet for the installation segment. Each aluminum foil was 15.2cm x 15.2cm in size and the end to end distance between two adjacent foils was 30.5cm.

The carpets are arranged in such a way that the wires get assembled to one location where the electronics setup has been made (see Figure 3.5 and Figure 3.6). All the wiring from one 32 sensor installation segment goes into one protoboard. The top layer of the sensor floor consisted of a sensor layer to which the multi-strand wires were soldered.

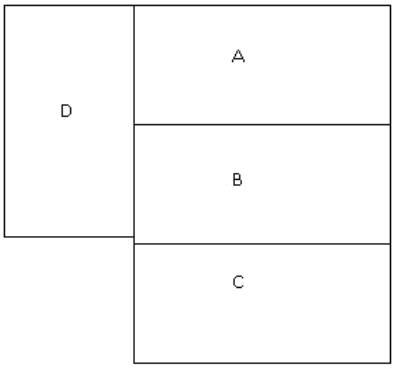

Figure 3.5: Figure indicates the arrangement of the 3.6m x 3.6m Installed Floor. Each of the installation segments A, B, C and D consists of 32 sensors arranged in 8 rows and 4 columns. All the wires from each sensor floor are routed to one location besides floor A.

Figure 3.6: Figure above is the sensor layer of the installed floor. The layout consists of 128 sensors placed in group of four installation segments consisting of 32 sensors arranged in 4x8 matrix formats. All the wires from the sensors are drawn to one location where the electronics unit was installed.

Figure 3.7: Top carpet layer of the sensor layout. The carpet is marked according to the installation segments laid underneath it. Segments A, B, C and D indicate the four installation segments from which the wires are drawn to a common location.

4.3. ELECTRONICS

This section describes the evolution and design of the amplifier used to signal condition the aluminum sensor output and make it compatible to be transferred to the micro-controller unit. The basic signal flow follows the block diagram mentioned in Figure 3.8.

4.3.1. Evolution of the amplifier

The aluminum foil sensors produced a noisy analog output voltage within a typical range when it was activated versus non-activated. The goal of the amplifier design was to convert this noisy signal from the aluminum foil into a noiseless digital signal. The aluminum foil has extremely high electrical conductivity (37.67 m/mm^2d) and the electrical resistivity is 2.65 μΩcm. The aluminum foil acquires energy that can be extracted but with a very low value of current flowing into the amplifier. This aluminum foil was connected as an input stage to the electronics section. It was essential to connect a very high value resistor with a buffer circuit at the input stage of the amplifier unit to prevent the loading effect. The resistor at the buffer stage would enable all the current coming from the foil sensor to be passed into the component (transistor, op-amp, etc).

The next stage of the electronics is to have the amplifier produce a HIGH output depending when the foil is activated. This HIGH output voltage signal can then be interfaced to a micro-controller unit. A HIGH input for a PIC 16F871 must be a voltage greater than 2.8V. There are many ways to achieve this goal.

One way is to design an open loop window detector circuit which detects when a signal is between two voltage thresholds and produces a HIGH output. Another approach uses a non-linear full wave rectifying circuit and an amplifier with direct analog to digital

conversion using available chips in the market is also a possibility. We choose to use the non-linear rectifying circuit as it has many advantages over the rest of the circuits.

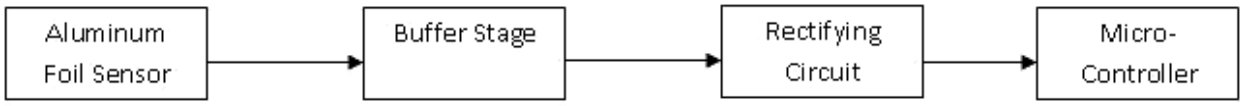

Figure 3.8: Block diagram summarizing the evolution and basic layout of the amplifier

Furthermore, we developed these amplifiers characterized by the sensor layout. We describe this evolution by discussing the design of three amplifiers.

4.3.2. 2x2 Development Floor Amplifier Design.

This amplifier design for the development board had first stage as a non-inverting unity gain buffer stage. A 30MΩ input resistor provided successful reproduction of the signal at the input stage of the amplifier. This was followed by a precision full wave rectifier stage followed by a non-inverting amplifier stage. All the three stages are built using one quad op-amp TL084CN (see appendix) whose slew rate is extremely high at 14V/μsec, providing high speed data capture and transmission. (See Figure 3.12 for final design).

3.3.2.1. Buffer Stage

The use of the buffer circuit lies in the fact that its input impedance is very high and the output impedance is almost zero. In our application, we already have an aluminum foil whose impedance is extremely high as an input source, and thus, we cannot connect the foil directly to the amplifier stages. The buffer is inserted between the high impedance aluminum foil and the rectifying circuit to perform an impedance matching between the two stages. The buffer stage (see Figure 3.9) draws negligible

current from the source (aluminum foil sensor) but, provides a current that is stepped up to match the rectifying circuit. With the gain of the buffer circuit adjusted to 1, it is a voltage follower circuit i.e. there is no gain or attenuation in the signal characteristics. The 10nF capacitor in parallel with the 30MΩ resistor shunts the high frequencies to ground while providing an open circuit for DC. It is important to note that no part of the input signal can be attenuated or modified until the rectification stage. Figure 3.9 is the schematic layout of the buffer circuit showing one of the 4 opamps in TL084.

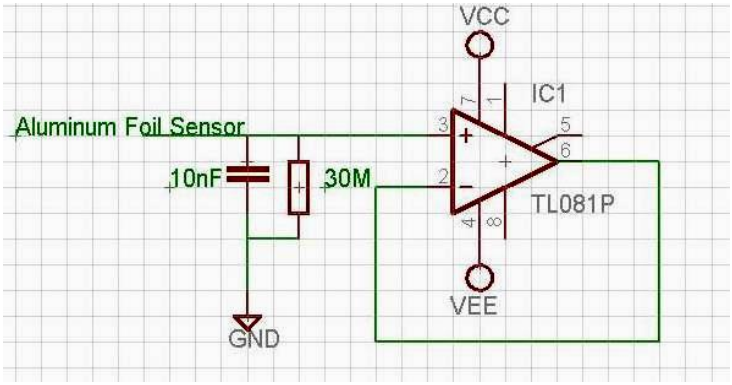

Figure 3.9: Buffer circuit displaying 30M input resistor. The input from aluminum foil is applied at pin 3 while the output is observed at pin number 6. The output fed back directly to the negative input, becomes a voltage follower with a gain of 1.

3.3.2.2. Precision Full Wave Rectifier

We designed a precision full wave rectifier circuit to handle the low level signal voltages from the aluminum foil (See Figure 3.10). Precision full wave rectifiers are non-linear applications of op-amp as they involve use of diodes in the design and take both the positive and the negative pulses, which the aluminum foil produced as a result of activation, and transmits one polarity and inverts the other. The precision full wave

rectifier avoids the forward voltage drop, V_F, typically 0.6V. In non-precision full wave rectification the signal must overcome at-least two diode drops. In the Figure 3.10, the full wave precision rectifier is implemented using an opamp, and includes the diode in the feedback loop. This effectively cancels the forward voltage drop of the diode, so very low level signals (well below the diode's forward voltage) can still be rectified with minimal error.

In our application, the input from the aluminum sensor is of the order of millivolt. The Figure 3.10 shows the schematic layout of the precision full wave rectifier circuit. Two op-amps, two diodes and five resistors are used to develop this circuit.

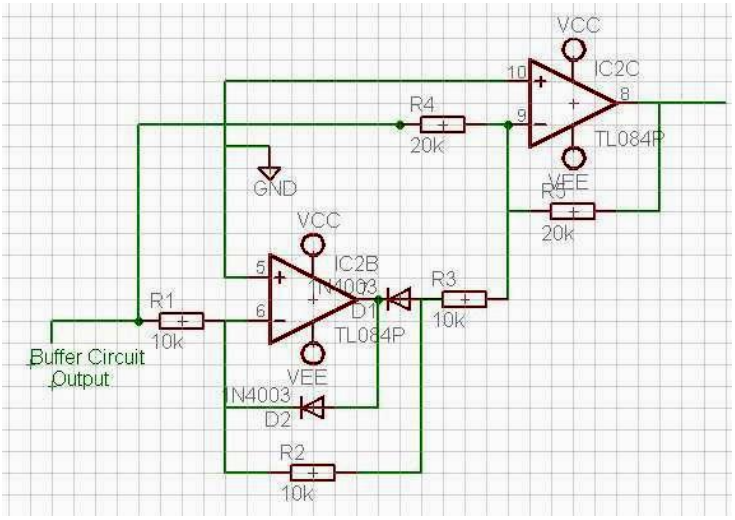

Figure 3.10: Precision Rectifier circuit with input from the buffer circuit. Output is observed at pin 8 of IC2C. The Precision Full Wave Rectifier uses D1 and D2 and that result is buffered by the unity gain amplifier I2C2.

In the Figure 3.10, the low frequency positive inputs produces 100% negative feedback since the diode D2 conducts and the forward voltage is effectively removed.

The inverting input pin of the opamp (pin 6) follows the positive half of the input signal almost perfectly. The transfer function is given by,

$$Vout = +Vin.\left(\frac{R2}{R1}.\frac{R5}{R3} - \frac{R5}{R4}\right) \qquad 3.1.$$

Where *Vout* is the output voltage observed at pin 8 of the TL084CN while *Vin* is buffer circuit output applied at pin 6.

For negative inputs, the opamp acts as an inverting amplifier and produces a positive voltage at the output. The transfer function is given by,

$$Vout = +Vin.\frac{R5}{R4} \qquad 3.2.$$

There is inherent asymmetry in the transfer functions for the two halves of the signal and the circuit can only work qualitatively provided that

$$\frac{R2}{R1}.\frac{R5}{R3} = 2.\frac{R5}{R4} \qquad 3.3.$$

Or

$$\frac{R2}{R1}.\frac{R4}{R3} = 2 \qquad 3.4.$$

From the above equations, it is observed that values and ratios of resistors R1 to R4 are important for satisfactory performance of this circuit. It also shows that there are two ways that the values could be arranged for precision rectification. One of these is to make R1, R2 and R3 all same value (R) and then make R4 and R5 equal to 2R for unity gain. The other is to make R1, R3, R4 and R5 the same value (R), and then make R2 equal to 2R. This also gives a unity gain. The effect of R5 in both cases is to apply an overall gain to the circuit. Its absolute value is not important so long as the condition given by Equation 4 is satisfied. This will only be the case if very close tolerance

resistors are used. The resistor values used are of high precision in order to keep the rectification process accurate with 1% tolerance in their values. A negative output can be observed by simply changing the orientation of the diodes.

3.3.2.3. Non-Inverting Amplifier

A non-inverting amplifier followed the precision full wave rectifier stage to amplify the millivolt signal for interface to the micro-controller unit. By adjusting the resistor values, a circuit having gain of 10 was designed, also, maintaining the polarity of the rectified signal. A 100k resistor is connected at the input of the non-inverting amplifier to prevent the output of the rectifier from getting loaded.

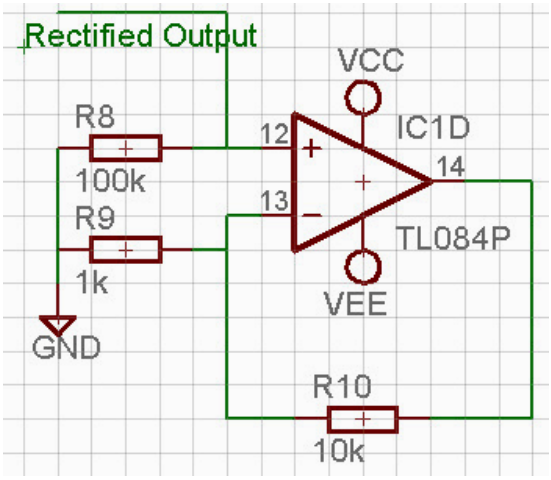

Figure 3.11: Non-Inverting amplifier circuit with rectified input applied at pin 12. This amplifier has a gain of 11, with the input resistance of 100kΩ.

For the output amplifier, output voltage is:

$$Vout = \left(1 + \frac{R10}{R9}\right).Vin \qquad 3.5.$$

Where *Vin* is the input from the rectifier circuit and *Vout* is the output of the amplifier. Thus, the gain of the circuit is 11. The complete schematic layout of the

amplifier is drawn in Figure 3.12. The performance of this amplifier is explained in the results section. A LM7805 and LM7905 (see appendix) voltage regulator was used to provide ripple free +5 V Vcc and –5V Vee respectively.

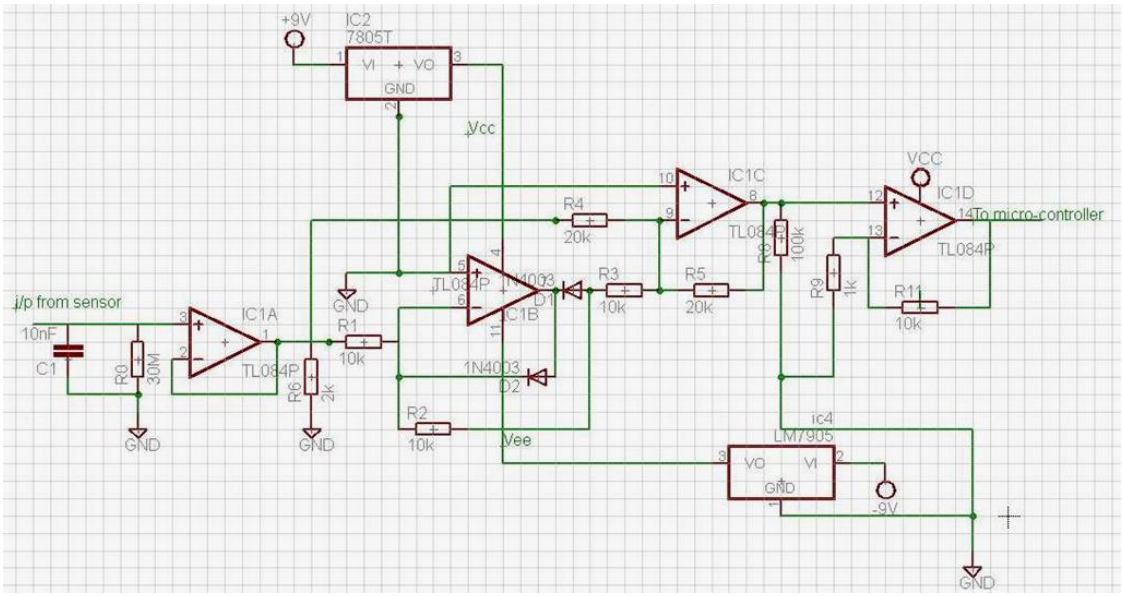

Figure 3.12: Complete Schematic Layout of the three stages; consisting of a buffer, full wave rectifier and the non-inverting amplifier. The three stages use all the amplifiers in the quad opamp chip, improving eventual packaging of the electronics.

Four amplifiers were connected to the four aluminum foil sensors and the output of these amplifiers was then interfaced with a micro-controller unit. Figure 3.13 indicates the protoboard of the complete amplifier circuit for the 2x2 development floor. The total cost of developing this protoboard is mentioned in the appendix.

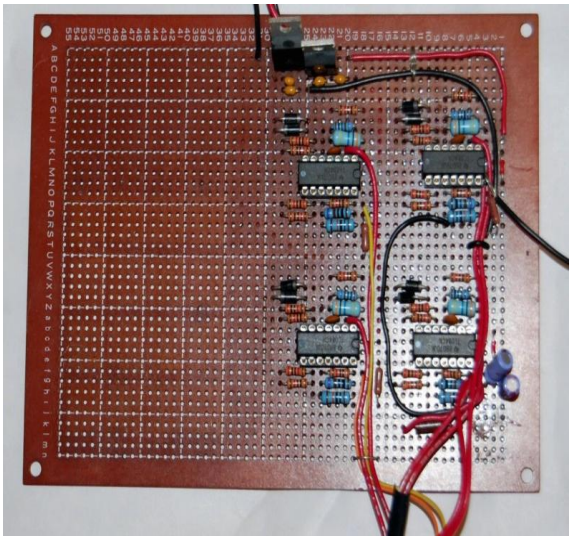

Figure 3.13: Protoboard for the complete 2x2 development floor amplifier design. The board contains four amplifiers connected to the four sensor inputs.

4.3.3. 7x3 Prototype Floor Amplifier Design.

Amplifier configuration similar to Figure 3.12 was utilized for developing the prototype floor amplifier design. This design contained 21 amplifiers connected to the 21 sensor foils. Since the sensors were arranged in 7x3 matrix format, a set of seven amplifiers were connected for each column. Three such sets of seven amplifiers were developed. In Figure 3.19, two-layered Printed Circuit Board layout for seven amplifiers designed using Eagle v5.6 software. Blue colored is the bottom layer and the red indicates top layer.

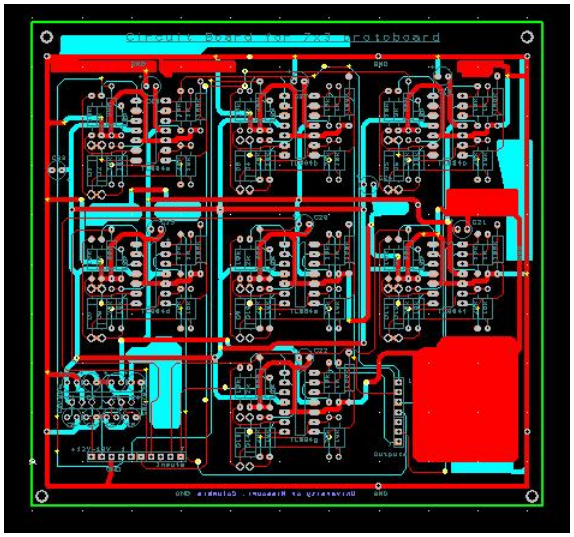

Figure 3.14: Printed Circuit Board layout for seven sensors in the 7x3 prototype board. This is a two layered board, the top layer is indicated by red color and the blue color indicates bottom layer. Three such Printed Circuit Boards were developed for the complete prototype board.

4.3.4. Electronics design for installed-floor carpet:

It was convenient to create several units of the 4x8 (32) sensors for the installed-floor carpet. A total of 132 sensors were used and covered by the installed-floor carpet. It was efficient to use analog multiplexers at the input for 32 sensors to reduce the electronics components in the circuit board. Four such circuit boards were made to accommodate the 132 sensors. The circuit design for 32 sensor system was different from the ones used for development and prototype faux floors. An 8:1analog multiplexer (CD4051) was used for each of the column in the 8x4 sensor system. Thus, for a 32 sensor system, four 8:1 multiplexers were used. The output lines of each 8:1 multiplexer were connected to one 4:1 (CD4052) multiplexer, and were followed by one precision full wave rectifier (PWR) circuit similar to Figure 3.12. The address lines of the multiplexers were selected by the microcontroller. It is known that the sensor foil has high output impedance. Such an input

signal cannot be interfaced with the comparatively low input impedance of the multiplexers. Hence, a buffer circuit similar to Figure 3.9 was connected at the input of the 8:1 multiplexers to provide impedance transformation and successful signal reproduction of the sensor foil at the multiplexer input. Instead of previously used TL084CN, a low quiescent current quad opamp MCP 6024 was used as a buffer. Figure 3.15 shows the block diagram for the 32 sensor electronics.

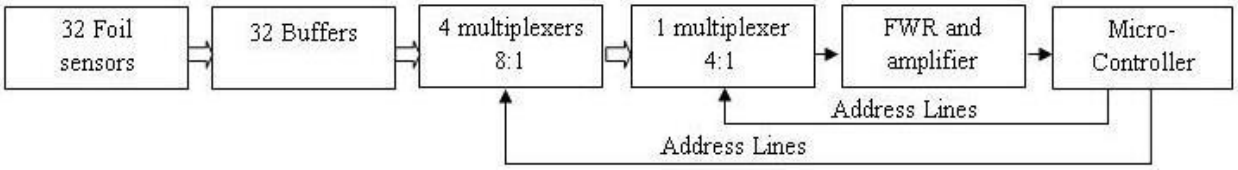

Figure 3.15: Block diagram describing the electronics design required to successfully detect and amplify the sensor input for the 32 sensor system. The buffer is given input from the aluminum sensor. The address lines to the multiplexers are selected by the micro-controller.

Thus, the complete circuit for 32 sensors consisted of 32 input buffers followed by the multiplexers and precision full wave rectifier. The circuit was powered by one +5V wall plug adapter; and this voltage were converted to +/- 9V by a dual output DC-DC converter NMH0509SC. The +/- 9V was stepped down using LM7805 and LM7905 voltage regulators to provide a Vcc and Vee of +5V and -5V respectively. NMH0509SC eliminated the need of a having a dual power supply for the circuit. Figure 3.16 shows the Printed Circuit Board layout for one 32 sensor system. Provision has been made to power up the micro-controller circuit using the +5V from the Printed Circuit Board. Figure 3.17 shows the illustrated diagram for one aluminum sensor input connected to one buffer opamp. 32 such inputs and buffer opamps are connected in the actual circuit.

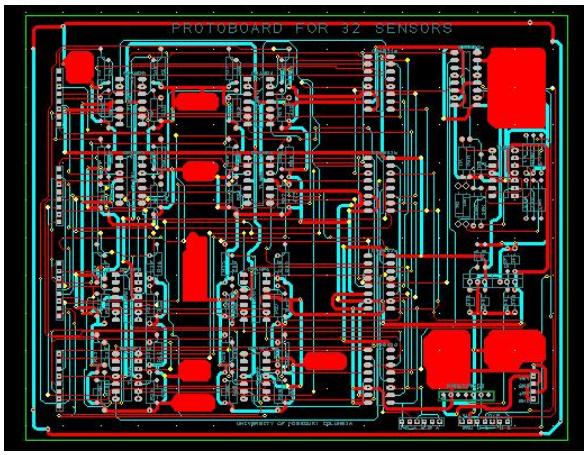

Figure 3.16: Protoboard for 32 sensor system. The circuit consists of 32 input buffers; four 8:1 multiplexers, one 4:1 multiplexer and only one precision full wave rectifier circuit. The complete circuit board is powered up using single +5V wall plug adapter. Four such protoboard were developed for the 128 sensor full carpet.

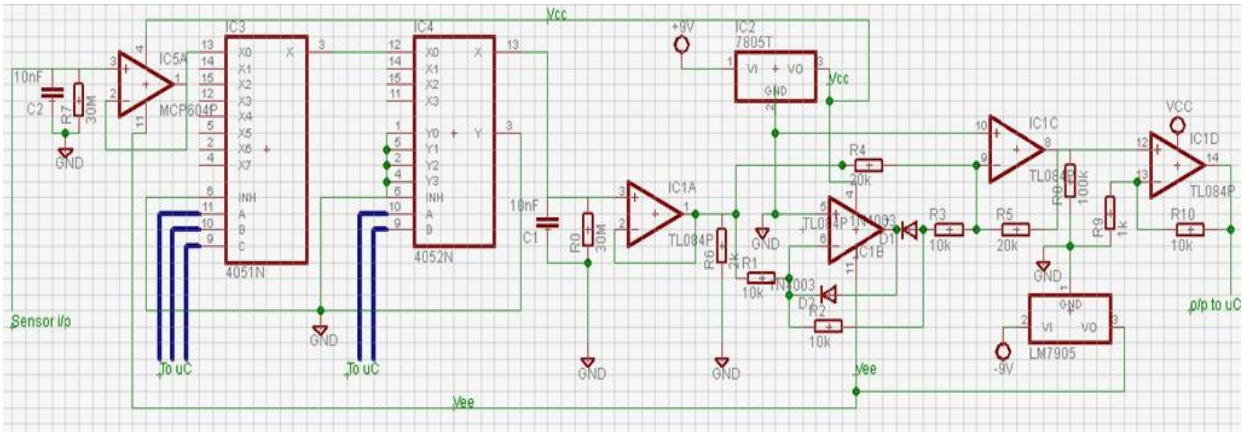

Figure 3.17: Schematic diagram illustrating single input from the aluminum sensor. It shows a single sensor buffer (MCP604P), one of the four 8:1 multiplexers (CD4051), the single 4:1 multiplexer (CD4052) and the four stage output amplifier servicing the first column of 8 sensors in the 8x4 array. All the components are powered using single power supply. The select lines of the multiplexers are controlled by the microcontroller unit. The output of the last amplifier (IC1D chip) is given to the microcontroller.

Designing printed circuit boards for the amplifiers, careful wire handling and the addition of a ground plane reduced the noise levels in the electronics unit. Using an aluminum box for placing the electronics unit also contributed in reduction of the noise interference.

4.3.5. Microcontrollers and Display electronics.

Apart from the analog electronics, a micro-controller was interfaced via serial communication to a PC for a computer display. One PIC16F871 microcontroller was used for both the development and prototype. However PIC18F4455 microcontrollers were interfaced to the analog circuit board for the full carpet system. Data among the four PIC18F4455 were transmitted wirelessly using Mi-Wi protocol. Display on computer was made using Java code. Figure 3.18 shows the general dataflow encompassing analog amplifiers, microcontroller unit (MCU) and the computer display.

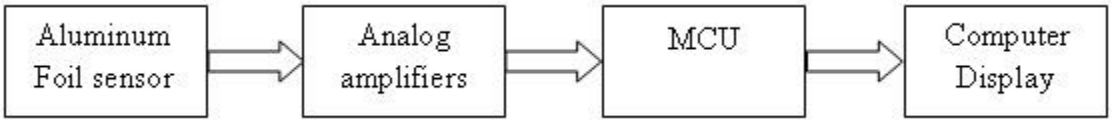

Figure 3.18: Block diagram indicating the final setup to test the performance of the aluminum sensors. This setup is common for the prototype floor, development floor and the full carpet.

TESTING: The output of the micro-controller unit was connected via a serial port to a computer unit where the sensor data was stored and displayed using Java code.

4.4. EXPERIMENTS:

Experiments were conducted on the prototype and the development sensor floor to determine its accuracy and the sensitivity. Whenever the foil was touched, we call it activated and when not touched, it's non-activated. A person stepped on and off the foil and at the same time, the output was noted on the oscilloscope and the computer display. Each time when the foil was activated, the computer display was expected to change its present color from green to red. When no person stepped on the foil, the monitor displayed green squares representing the arrangement of the sensor floor. Thus, the monitor display had 4 squares for prototype sensor floor and 21 squares for the development sensor floor. The experiments were categorized to determine the following activities.

4.4.1. Comparison of the output voltages of the aluminum foil sensor when activated.

This experiment aimed to determine the maximum change in the output voltage in the aluminum foil sensor when activated. A 30.5cm x 30.5cm (12in x 12in) aluminum foil was connected directly to the oscilloscope and was randomly activated by stepping on it. The voltages were observed on the Hewlett Packard oscilloscope. The aluminum foil sensor did not contain any ground plane or any plastic underneath it. The experimental setup was similar to Figure 3.19.

4.4.2. Sensor activation and performance in the presence of lights.

We detected the performance of the aluminum sensors in the presence of stray electromagnetic energy ubiquitously available in the environment. This included mostly 60Hz power line, energy from electrical and laboratory equipment, computer systems, etc.

For this experiment, only 1 sensor was connected directly to the oscilloscope. Initially, all the lights and the electrical instruments in the laboratory (example: oscilloscopes, power supplies, function-generator, etc) were kept ON. The activation of the aluminum foil was noted using the oscilloscope reading. Similarly all the equipments, the lights and the electrical instruments were turned OFF and the observation was made. The block diagram of the setup is drawn in Figure 3.19.

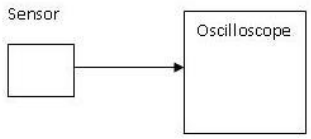

Figure 3.19: Setup arrangement to determine the characteristics of the aluminum foil sensor in presence of electromagnetic components such as laboratory instruments, tube-lights, etc. The observations with activation of foils are made with the laboratory instruments ON and OFF.

4.4.3. Variance in the performance of the sensors on prototype floor with change in their sizes.

The aim of this experiment was to detect the effect the performance of the sensor floor with the variation of the sensor size. Three sensor sizes 7.6cm x 7.6cm (3in x 3in), 15.2cm x 15.2cm (6in x 6in) and 30.5cm x 30.5cm (12in x 12in) were used on the development system. Each sensor was placed in the lower left hand of a box 30.5cm (12in) squared and the size of the sensor was changed. The arrangements of the aluminum foils were similar to those in. Sensors A, B, C, and D of the three sets of size were covered with carpet and stepped on and off 50 times with the software filter ON. We noted the detection of stepped signal was sensed by the electronics unit. The performance of the sensors was determined by categorizing the readings into four sets;

true positive, true negative, false positive and false negative. The definitions of these terms with respect to our application are specified in the results section. Later, the ROC space characteristics depending on these parameters were plotted. The aluminum sensors were connected interfaced with the microcontroller, followed by the computer display. An oscilloscope was connected to the output port of the microcontroller for debugging purposes. The block diagram of the experimental setup is drawn in Figure 3.20. A note was made when the aluminum foil was sensed by the electronics setup.

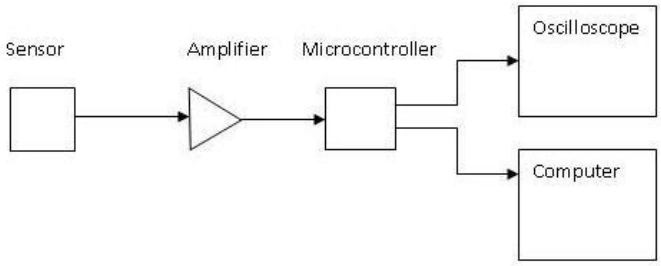

Figure 3.20: Setup block diagram for the prototype sensor floor to determine performance with variation of the sensor size. The micro-controller output was connected to both the oscilloscope and the desktop computer.

4.4.4. Performance of the Development System using 30.5cm x 30.5cm aluminum foil with and without the Software Filter.

We assessed the performance of the development system with and without the application of the Software Filter with the 30.5cm x 30.5cm sensors. Readings were observed for 50 steps on and off the sensor. The software filter was then removed and the experiment was repeated again for 50 steps. Like the previous test, we checked if the stepped signal was sensed by the electronics unit and the observations were categorized

into four sets; true positive, true negative, false positive and false negative. The ROC space characteristics for both, with and without filter were plotted and compared. The experimental setup for this test was similar to Figure 3.20.

4.4.5. Amplifier Performance on the Development Board.

Each stage of the three-stage non-linear amplifier was tested for its performance using the development system. The buffer stage was initially tested to check if the aluminum foil input was successfully reproduced. Oscilloscope probes were connected to the input and the output of the buffer and the signals were compared on two channels on the oscilloscope. The output of buffer was then tested for rectification using the precision full wave rectifier. It was worthwhile to check if the negative pulses were being successfully rectified as it contained the data when a person took his foot from the aluminum foil. Lastly, the gain stage of the amplifier was tested to check if the opamp was saturated to its maximum possible value. The aluminum foils were activated momentarily and two oscilloscope probes were connected; one at the input and other probe at the output pin of the gain stage. The signal levels were checked when a person activated and de-activated the aluminum foil. The amplifiers were powered by a supply voltage of +/- 9V with maximum load current of 1A. The block diagram of the test setup is shown in Figure 3.21. No microcontroller interface was required to carry out these tests.

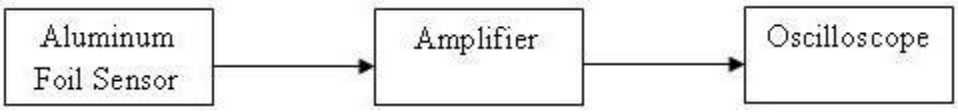

Figure 3.21: Block diagram for the setup used to test all the three stages in the amplifier. No microcontroller interface was necessary for this test. The buffer, full wave rectifier and the gain stages were tested and observed on the oscilloscope.

4.4.6. Performance of the 21 sensor prototype system.

The setup for testing performance of prototype system is similar to Figure 3.20. Figure 3.22 indicates the electronics board which performs the analog to digital conversion of the sensor signal and passes it to a computer database. The figure consists of an analog amplifier, microcontroller unit and a serial unit to transmit the data to the computer. This experiment aimed at determining the performance of the system for a higher number of sensors, and the distance between two sensors was reduced in comparison with the 2x2 development floor. The size of each sensor was 15.2cm x 8in and the spacing between two adjacent sensors was 15.2cm. Important factors like the amount of power consumed, crosstalk between adjacent sensors, and effect of noise on the system due to increase in the number of sensors were to be observed. Each of the 21 sensors in the development system was activated for 5 seconds by stepping on it. Care was taken that at a given time, only one sensor was activated and the change in the monitor display was noted. Corresponding to each step, the number of data samples passed via the serial port to the display computer were measured and saved in an excel sheet.

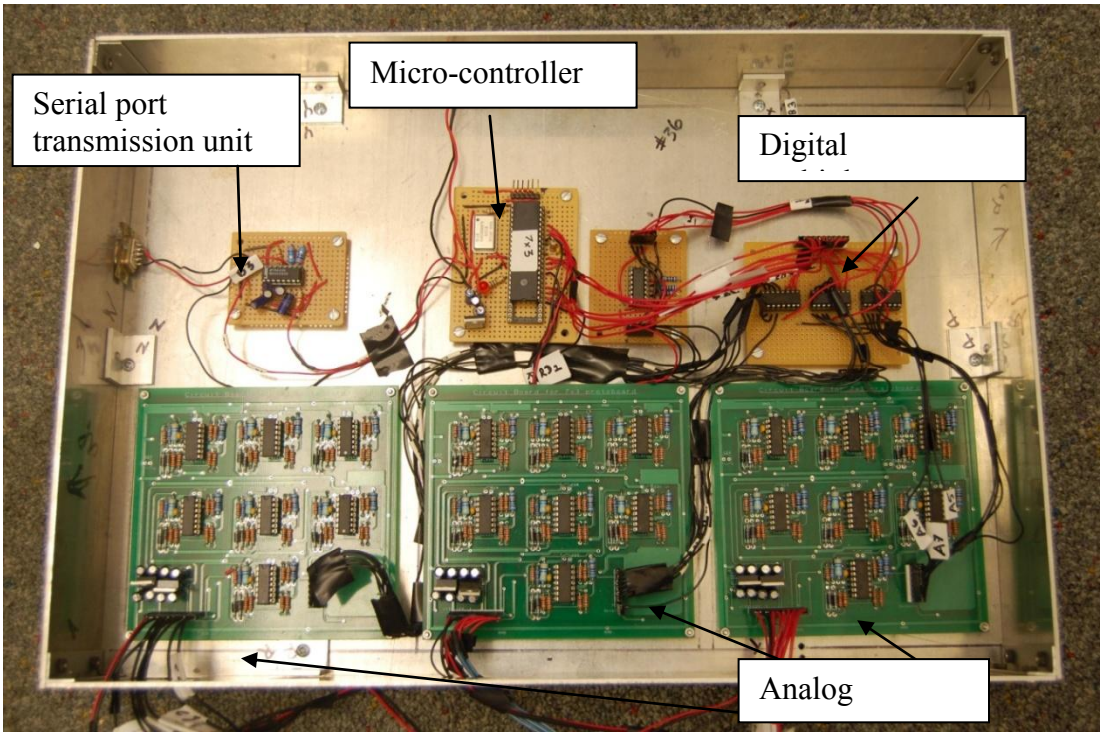

Figure 3.22: The electronics board containing the analog to digital conversion of the sensor signal. The green color boards are the analog amplifier which performs the signal rectification and amplification. The micro-controller then transmits sensor signal via the serial cable to a stationary computer.

4.4.7. Performance of the installed – floor.

We conducted a test procedure to measure the performance of the installed floor similar to the test carried out to measure the performance of the prototype system. At a given time, only one sensor among the 132 sensors on the installed floor was activated for 5 seconds.

The test setup was similar to Figure 3.20. The installed floor system contained four 8x4 installation segments. A set of analog amplifier and microcontroller was connected to each of the four installation segments. Thus, the complete setup included four analog amplifier set, four microcontroller units and one PC. The microcontrollers formed a peer-peer network and only one of the four microcontrollers was connected to

the PC via serial communication. The analog amplifiers were powered using a +5V wall plug adapter. The number of pulses that were generated by an activation on the sensor was recorded in an excel sheet. We intended to measure the false positives that were generated when one particular sensor was activated.

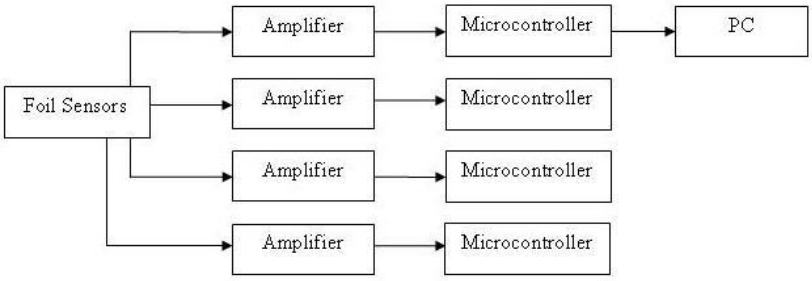

Figure 3.23: Setup to formulate the performance of the installed floor system. Only one among the four peer- peer connected microcontrollers is connected to the PC via serial communication. A +5V wall plug adapter is used to power up the electronics unit.

4.4.8. Amplifier Performance on the 4x8 Installation Segment and the Installed Floor.

Two tests to check the performance of the amplifier circuit were carried out; one on the 4x8 Installation Segments and the other was carried out on the installed floor. 32 aluminum foil sensors connected to the amplifier circuit followed by one PIC 16F871 microcontroller and the computer display. The select lines of the multiplexer were interfaced with the micro-controller and hence, it was important to determine the scanning rate at which the select lines would be altered so that all the movements on the floor would be successfully captured and reproduced. Once the scanning rate was determined (15), a test to determine the output of the amplifier was performed. The setup for the test was similar to Figure 3.18. The aluminum foils were momentarily excited

and the output was observed on the display. The complete circuit was powered from a single +5V power supply with 1A current output.

Next, the amplifier response for the complete installed floor was measured. Four Printed Circuit Boards were connected to the four installation segments and each of them was followed by micro-controller unit. The system ground was connected to the earth pin from the AC mains in order to achieve better ground. It was important to observe the amount of current conceived by the amplifier circuit, its performance in presence of static charges generated due to large number of aluminum foil sensors, the response time of the electronics unit and the repeatability of the performance of electronics over a period of time.

CHAPTER 4 : RESULTS

4.1 **Comparison of the output voltages of the aluminum foil sensor when activated.**

The results displayed in Figure 4.1were obtained when a 30.5cm x 30.5cm sensor foil was activated. The voltages were observed on Hewlett Packard 54602B oscilloscope. A minimum voltage of 31.6 millivolts was observed for sensor D without the activation of the foil and a minimum of 144 millivolts was observed for sensor C upon activation of the aluminum foil. A minimum rise of 200% was observed between the activation and non-activation of the aluminum foil.

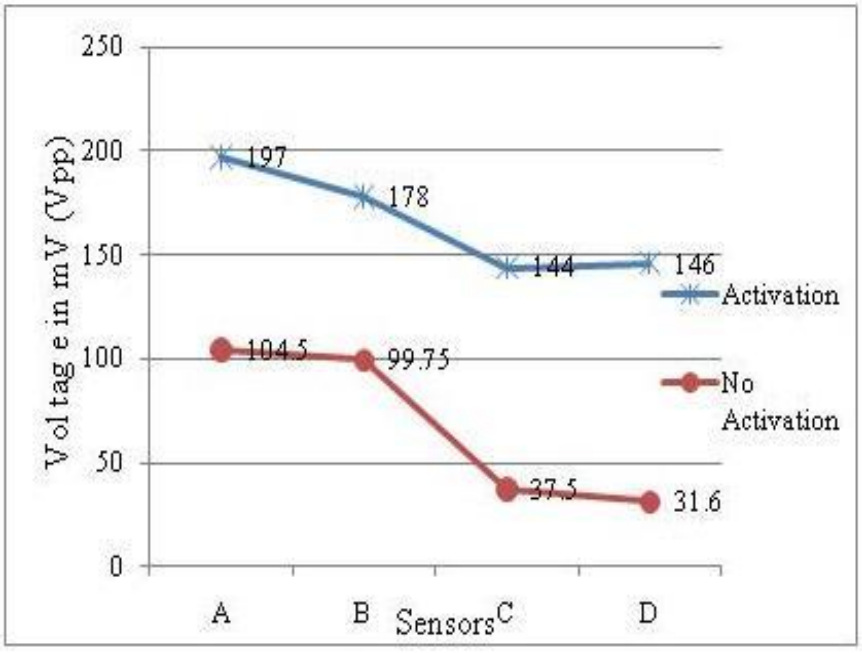

Figure 4.1: The sensor axis labeled as A, B, C, and D represents the particular sensor excited and the ordinate axis represents the voltages of the difference in millivolts observed on oscilloscope. The minimum difference in the output between the two conditions is 200%.

4.2 **Sensor activation and performance in the presence of lights.**

In Figure 4.2 the sensors axis represents the three sizes (7.6cm x 7.6cm, 15.2cm x 15.2cm and 30.5cm x 30.5cm) of the aluminum foil in terms of its area. The ordinate represents the peak-peak output voltage in terms of millivolts. It is observed that the increase in the voltage from 22.9 square cms to 91.4 square cms is approximately 72% and that of 91.4 square cms to 365.8 sqaure cms is approximately 74%. Hence the observations follow an exponential curve in correspondence to the increase in voltages as opposed to the increase in the size of the sensor. The maximum increase in the sensor size is 44%. These co-ordinates are then joined by an exponential curve.

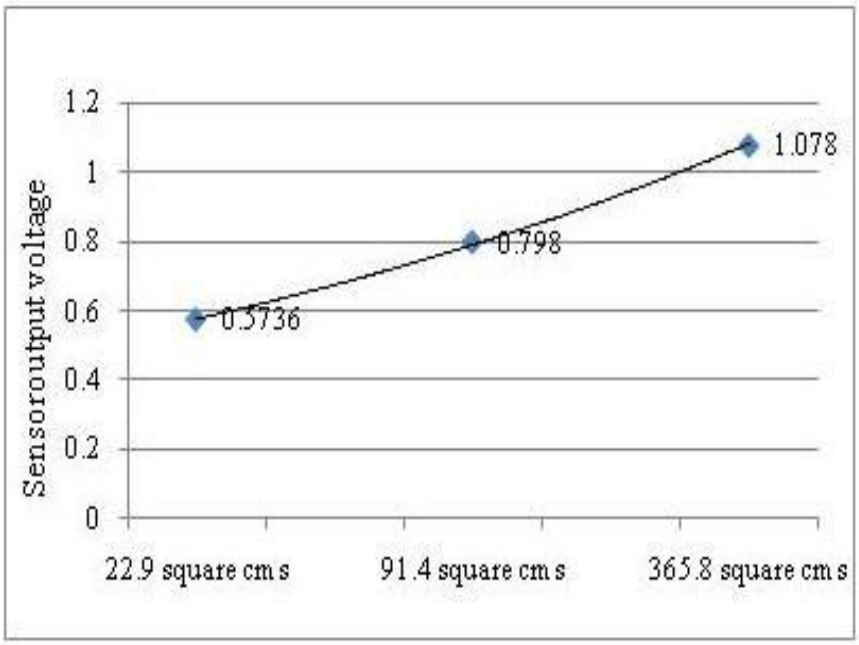

Figure 4.2: Abscissa represents the sensor area against the output voltage on the ordinate axis. The co-ordinates are joined by an exponential curve indicating that the rise of voltages is almost exponential to the rise in the area of the sensors.

In Figure 4.3 comparision is made between lights ON and lights OFF for all the 3 sizes of sensors. It is observed that the output voltage increases when the lights are ON not only for 1 sensor but for all sizes. The difference in the voltages with lights ON and OFF is approximately 70%.

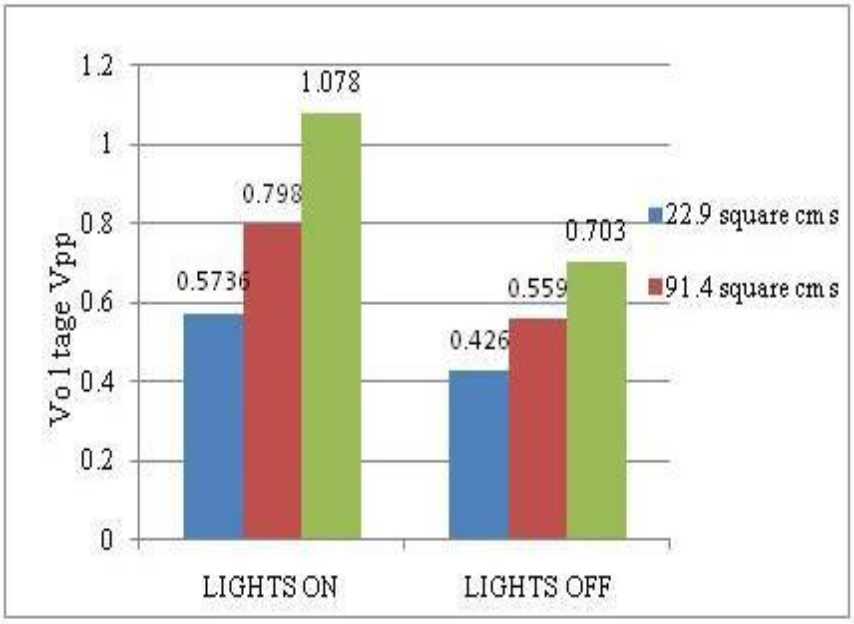

Figure 4.3: The abscissa indicates the situation whether the lights in the room were ON or OFF. The voltages corresponding to these situations are noted in millivolts on the voltage axis.

4.3 Variance in the performance of the complete system (including sensors and electronics) using development floor with a change in sensor size.

A test was carried out to characterize the performance of the development system based on three aluminum foil sizes; 7.6cm x 7.6cm, 15.2cm x 15.2cm and 30.5cm x 30.5cm. A more comprehensive test was to determine the performance

matrix for all of these tests. The true positive rate, false positive rate and the accuracy are evaluated using:

True positive Rate = True Positive/ Number of samples

False Positive Rate = False Positive/Number of samples

False Negative Rate = False Negative/Number of samples

Accuracy = (True Positive + True Negative)/ (Sum of column elements in confusion matrix)

True positive condition is observed when the foil was activated and the corresponding RED display was observed on the monitor screen. A true negative is observed when the foil was not activated, and the monitor screen showed no change in its color. Similarly, false positive is defined the condition when the foil was not activated, but the monitor screen displayed RED color indicating activation. This condition is equivalent to a 'false alarm' situation. Lastly, false negative is observed when the sensor is activated and no display is seen on the monitor screen. False negatives are crucial and equivalent to a 'miss' condition.

Table 4-1 and Table 4-2 shows the performance of the 7.6cm x 7.6cm aluminum foil. The accuracy, false positive rate (FPR), true positive rate (TPR) and false negative rate (FNR) for each of the foils is calculated using the above formulae. The average TPR is low at 85.5% indicating that not all of the sensor activation is captured by the electronics setup. The number of misses (average FNR) is high (14.5%); however, the system is highly accurate (92.75%) and produces no false alarms (average FPR). The true positive, false positive and false negative values were measured during the tests, while the true negative values were calculated.

Table 4-1 Table indicating performance of the development system with 7.6cm x 7.6cm aluminum foil and each of the A, B, C, and D aluminum foils were activated 50 times.

Performance of development system with 7.6cm x 7.6cm foil								
Foil steps = 50 each	**MEASURED**			**CALCULATED**				
	True Positive	False Positive	False Negative	True Negative	Accuracy (%)	TPR (%)	FPR (%)	FNR (%)
Foil A	35	0	15	50	85	70	0	30
Foil B	45	0	5	50	95	90	0	10
Foil C	46	0	4	50	96	92	0	8
Foil D	45	0	5	50	95	90	0	10

Table 4-2: The two crucial parameters; average false negative rate (misses) obtained for this system is very high (14.5%) and the true positive rate (condition when activation on the foil is captured by the electronics system) are very low (85.5%).

Average Accuracy (%)	92.75
Average TPR (%)	85.5
Average FPR (%)	0
Average FNR (%)	14.5

Table 4-3 and Table 4-4 show the performance matrix for development system with 15.2cm x 15.2cm sensors system. The total accuracy of this sensor system is 97.25%. The average false alarms (FPR) generated by the foils are very low at 0.5% and percentage of misses (FNR) is considerably low at 5%. 95% of the sensor activation was successfully detected by the electronics system indicated by the average TPR. The average accuracy and detection of foil activation rose by 4.5% and 9.5% respectively; and the average misses dropped by 9.5% for the 15.2cm x 15.2cm aluminum foil as compared to the 7.6cm x 7.6cm aluminum foil.

Table 4-3: The table below indicates performance of the development system with 15.2cm x 15.2cm aluminum foil and each of the A, B, C, and D aluminum foils were activated 50 times.

Performance of development system with 15.2cm x 15.2cm foil								
Foil steps = 50 each	**MEASURED**			**CALCULATED**				
	True Positive	False Positive	False Negative	True Negative	Accuracy (%)	TPR (%)	FPR (%)	FNR (%)
Foil A	47	1	3	49	96	94	2	6
Foil B	47	0	3	50	97	94	0	6
Foil C	47	0	3	50	97	94	0	6
Foil D	49	0	1	50	99	98	0	2

Table 4-4: The average accuracy, TPR of these foils is very high at 97.25% and 95% respectively. The false alarms (FNR) and misses (FPR) are considerably low at 5% and 0.5% indicating better foil performance with respect to increase in size

Average Accuracy (%)	97.25
Average TPR (%)	95
Average FPR (%)	0.5
Average FNR (%)	5

Table 4-5 and Table 4-6 show the performance matrix for development system with 30.5cm x 30.5cm aluminum foil. The total accuracy of this sensor system is 98%. The false alarm (false positive) generated by this system is zero and percentage of miss (false negative) is very low at 4%. 96% of the sensor activation is successfully detected by the electronics system indicated by the true positive. The accuracy and the true positive rates for 30.5cm x 30.5cm have been improved by almost 2% as compared to the 15.2cm x 15.2cm.

Table 4-5: Performance matrix for development system with 30.5cm x 30.5cm sensors drawn with 50 samples of activating the aluminum foil.

Performance of development system with 30.5cm x 30.5cm foil with FILTER ON								
Foil steps = 50 each	**MEASURED**			**CALCULATED**				
	True Positive	False Positive	False Negative	True Negative	Accuracy (%)	TPR (%)	FPR (%)	FNR (%)
Foil A	48	0	2	50	96	94	2	6
Foil B	50	0	0	50	97	94	0	6
Foil C	50	2	0	48	97	94	0	6
Foil D	47	0	3	50	99	98	0	2

:

Table 4-6: The average accuracy, TPR of these foils is highest at 98.25% and 97.5% respectively. The false alarms (FNR) and misses (FPR) are lowest at 2.5% and 1% indicating even better foil performance

Average Accuracy (%)	98
Average TPR (%)	97.5
Average FPR (%)	1
Average FNR (%)	2.5

Table 4-7 and Table 4-8 show the confusion matrix for 30.5cm x 30.5cm aluminum foil with the software filter OFF. Though the TPR for this test was considerably high 97%, the average accuracy was very low at 85.5%. The average false alarm (FPR) generated by these tests were very high at 26%. Due to the removal of the filter, there were very less misses (FNR) in the system. As compared to the foil performance with the filter ON, the accuracy reduced by 12.75% and the false alarms generated increased by 25%.

Table 4-7 : Performance matrix of the development system using 30.5cm x 30.5cm aluminum foil with the SOFTWARE FILTER OFF.

Performance of development system with 30.5cm x 30.5cm foil with FILTER OFF								
Foil steps = 50 each	**MEASURED**			**CALCULATED**				
	True Positive	False Positive	False Negative	True Negative	Accuracy (%)	TPR (%)	FPR (%)	FNR (%)
Foil A	47	5	3	45	92	94	10	6
Foil B	50	10	0	40	90	100	20	0
Foil C	50	17	0	33	83	100	34	0
Foil D	47	20	3	30	77	94	40	6

Table 4-8: The accuracy of the system is reduced and the percentage of 'false alarm' generated is increased as compared with the performance of 30.5cm x 30.5cm with the FILTER ON.

Average Accuracy (%)	85.5
Average TPR (%)	97
Average FPR (%)	26
Average FNR (%)	3

A representation in ROC space helps to appreciate the high degree of accuracy that the system provides in detecting foil activity. The performance variance of the sensor system with respect to the change in size is shown in Figure 4.4. The ROC space gives a comparison between the true positives and the false positives of any system. The true positive rate is equivalent with the sensitivity of the system and false positive rate is equivalent with the false alarm rate.

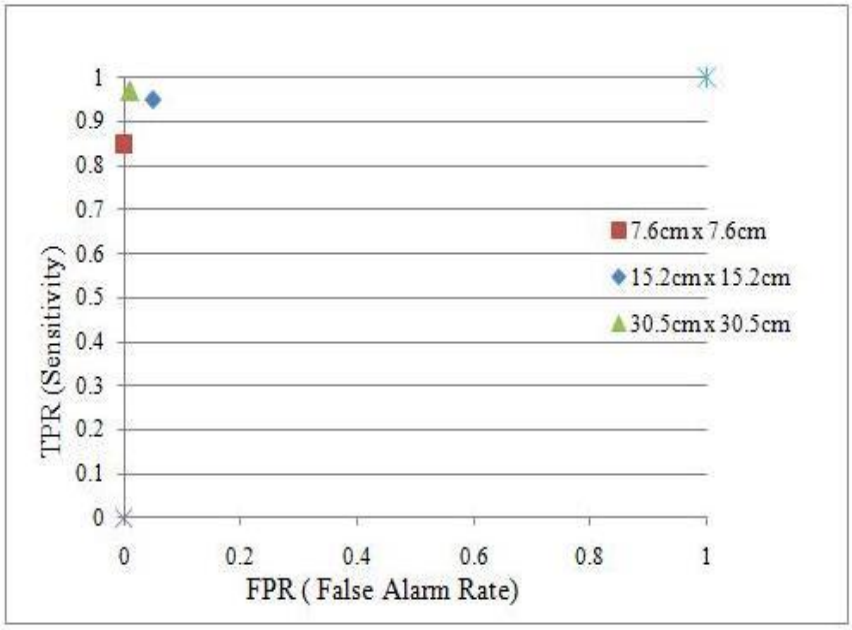

Figure 4.4: ROC space for complete development system with 7.6cm, 15.2cm and 30.5cm aluminum foils. The data was sampled with the filter ON. All the points lie almost on the ordinate axis indicating highly efficient and reliable system performance. The sensitivity improves as the size of the sensor increases.

4.4 Performance of the development system using 30.5cm x 30.5cm with and without the Software Filter.

Figure 4.5 represents the graphical comparison of the effect of the Software Filter on the performance of the development board for 30.5cm x 30.5cm sensor. The true positive rate is compared with respect to both the false positive rate (false alarms) and the false negative (misses) rate. An increase in the false alarm has been observed with the omission of the software filter.

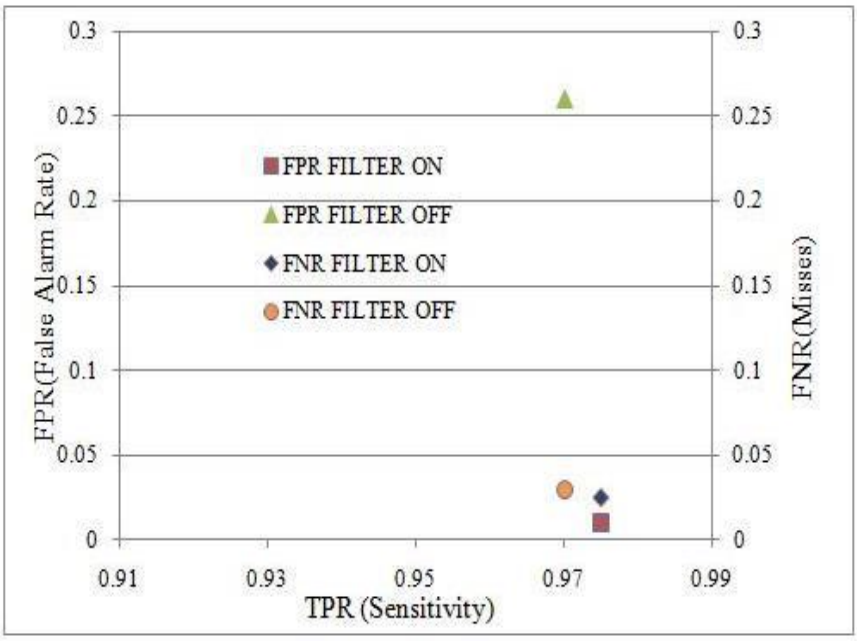

Figure 4.5: Performance of the development system 30.5cm x 30.5cm aluminum foils in the presence and absence of the software filter. The graph contains two vertical axes FPR and FNR; each plotted against the corresponding TPR value. High values of false alarms (FPR = 0.26) are observed when the software filter is turned OFF.

4.5 **Amplifier Performance on the Development Board.**

The amplifier designed is a non-linear amplifier which rectifies the signal and then amplifies it by a factor of 11. The supply voltages are given as +/- 5V and hence the saturating output voltage is observed around +5V. As the op-amp is not a rail to rail op-amp, the maximum output voltage obtained was approximately 4.2V (see Figure 4.6) when the aluminum foil was activated. A minimum voltage of approximately 200-300millivolts was observed when the foil was not activated. The amplifier response to the excitation of the sensor was observed without any delay, producing a HIGH voltage instantly. The gain of 11 drove the amplifier output to saturate at the maximum voltage, sufficing the necessity to interface with the micro-controller unit. Each op-amp in the quad TL084 consumed a maximum quiescent current of 2.34mA. 9.36mA current was consumed by one quad op-amp and since the circuit contained four quad op-amps, a maximum of 37.44mA current was drawn.

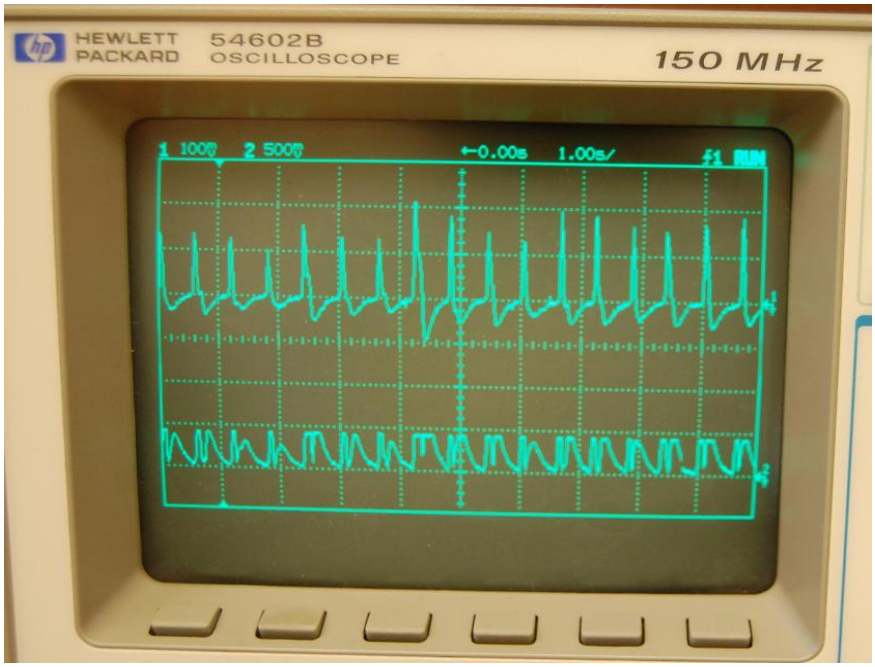

Figure 4.6: The picture displays the output of the amplifier against the sensor output. The probe used for channel 2 is a 10:1 probe with the voltage/division scaling 500millivolts/division. The maximum output voltage obtained was approximately 4.2V when the aluminum sensor was activated and when not activated, the output voltage was approximately 0V.

4.6 **Performance of the 21 sensor prototype system.**

Figure 4.7 displays the performance of the 7 x 3 prototype system. This graph is an average of the three sets of the readings taken. In this test, we have measured the count of the data samples transmitted by microcontroller to the computer in 5 seconds. Also, the false positives were observed and noted during the excitation of a particular sensor. The maximum false positive is obtained for column C4 which is approximately 23.7%. 33% of the sensors did not have any false negatives. Out of the remaining 67%, the average percentage of the false negatives was only 5.26% of the total number of counts. The least number of counts were obtained for column C1 (1273). An average of 1300 counts was observed to be transmitted from the micro-controller to the display computer.

	A1	A2	A3	A4	A5	A6	A7	B1	B2	B3	B4	B5	B6	B7	C1	C2	C3	C4	C5	C6	C7
A1	5430	33	0	0	0	0	0	0	0	0	0	0	0	0	0	37	0	0	0	0	0
A2	37	3236	0	0	0	0	0	0	0	0	0	0	0	0	0	0	0	0	0	0	0
A3	0	291	3476	0	0	0	0	0	0	0	0	0	0	0	0	0	0	0	0	0	0
A4	0	0	0	2642	0	0	0	0	0	0	0	0	0	0	0	0	0	0	0	0	0
A5	0	0	0	0	3818	0	0	0	0	0	0	0	0	0	0	0	0	0	0	0	0
A6	0	0	0	0	30	3496	0	0	0	0	0	0	0	0	0	0	0	0	0	0	0
A7	0	0	0	0	0	52	4746	0	0	0	0	0	0	0	0	0	0	0	0	0	0
B1	0	0	0	0	0	0	0	5293	0	0	0	0	0	0	0	105	0	0	0	0	0
B2	0	0	0	0	0	0	0	0	4253	0	0	0	0	0	0	518	0	0	0	0	0
B3	0	0	0	0	0	0	0	0	0	5219	0	0	0	0	0	0	0	0	0	0	0
B4	0	0	0	0	0	0	0	0	0	0	4681	0	0	0	0	0	0	0	0	0	0
B5	0	0	0	0	52	0	0	0	0	0	0	5586	0	0	0	0	0	0	0	0	0
B6	0	0	0	0	0	0	0	0	0	0	0	0	2898	0	0	0	0	0	0	0	0
B7	0	0	0	0	0	0	43	0	0	0	0	0	73	4778	0	0	0	0	0	0	121
C1	0	0	0	0	0	0	0	0	0	0	0	0	0	0	1271	0	0	0	0	0	0
C2	0	0	0	0	0	0	0	0	0	0	0	0	0	0	0	5692	0	0	0	0	0
C3	0	0	0	0	0	0	0	0	0	0	0	0	0	0	0	0	4077	0	0	0	0
C4	0	0	0	0	0	0	0	0	0	0	0	0	0	0	0	0	705	2970	0	0	0
C5	0	0	0	0	0	0	0	0	0	0	0	0	0	0	0	0	0	35	4061	0	0
C6	0	0	0	0	0	0	0	0	0	0	0	0	0	261	0	0	0	0	0	5124	0
C7	0	0	0	0	0	0	0	0	0	0	0	0	0	0	0	0	0	0	0	281	3524

Figure 4.7: Graph displaying the performance of the prototype system when an individual foil sensor was excited amongst the array of 21 sensors. The rows and columns are marked in array format from A1 to C7 indicating the actual sensors on the development system. The diagonal elements indicate the excited sensors against the false negatives otherwise noted in the rows and columns. The maximum false negatives are obtained in column C4 which is approximately 23.7%

Figure 4.8 indicates the normalized representation of the data obtained in Figure 4.7. By normalizing, we make all the diagonal elements are rounded to the maximum value observed and the corresponding false negative values are calculated with respect to this maximum normal value. From Figure 4.7, it is found out that the maximum count value is observed for C2 (5692). Hence, all the diagonal elements are rounded off to 5692 and the error percentages are calculated with respect to 1865. The abscissa in the graph below indicates the aluminum sensors and the ordinate axis displays the percentage of false negatives obtained.

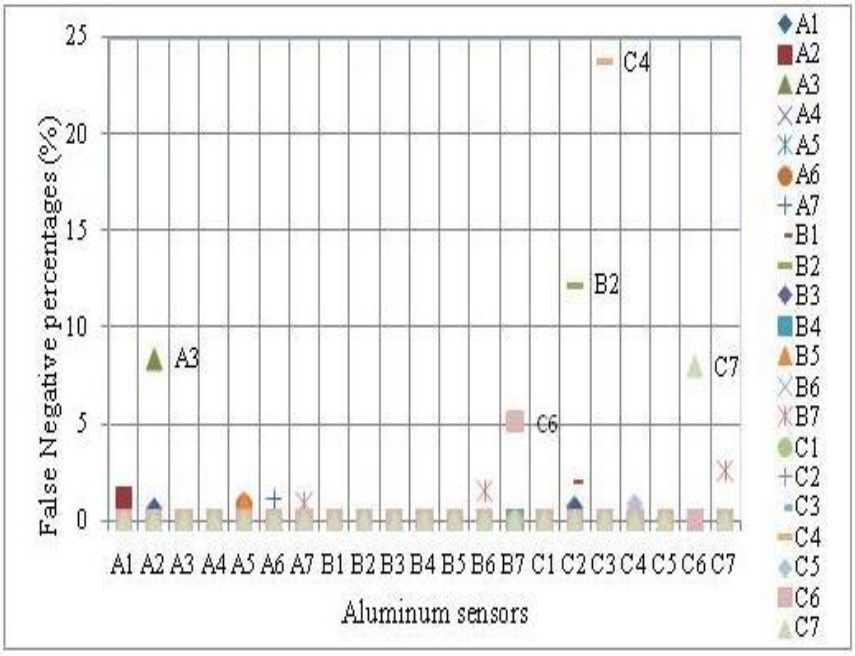

Figure 4.8: Figure indicating the percentage of the false negatives observed in the Prototype System when individual sensors were activated for 5 seconds. The colored symbols indicate the particular sensor type and its percentage of false negatives. The maximum false negative percentage was obtained for C3 which is approximately 23.737%.

4.7 **Performance of the installed – floor.**

Tests were carried out to observe the performance of the installed floor following similar procedure as the prototype system. Error percentage in terms of the false positives were obtained for the 128 sensors in the installed floor and plotted. Figure 4.9, Figure 4.10, Figure 4.11 and Figure 4.12 indicate the graphs drawn for the installation segments A, B, C and D. It is observed that the false positives obtained in each of the installation segment are very low as compared to all the other systems.

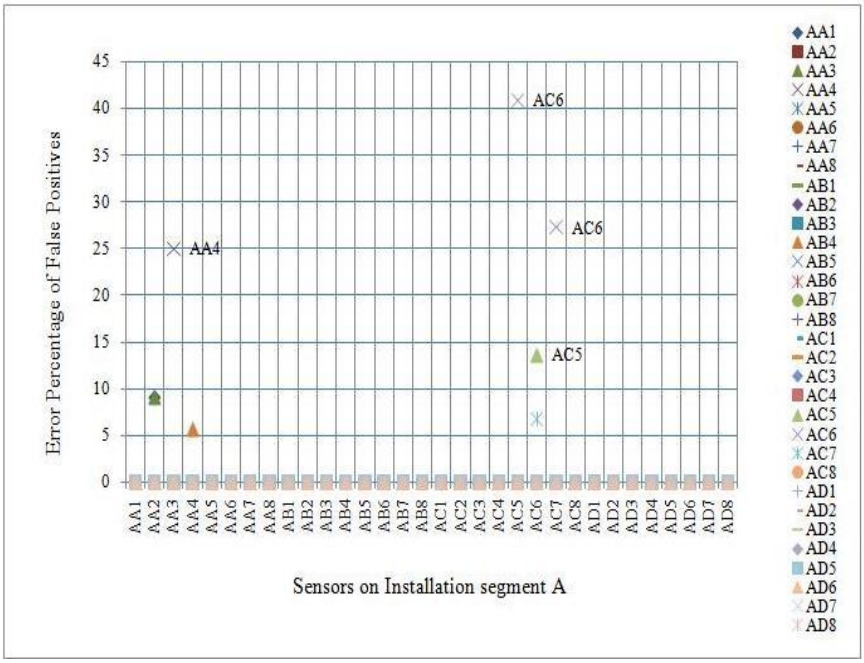

Figure 4.9: Figure displaying the error percentage of the false positives for the installation segment A. The maximum error rate was observed to be approximately 42% for the sensor AC5. The average error rate for all the 32 sensors was 0.134%.

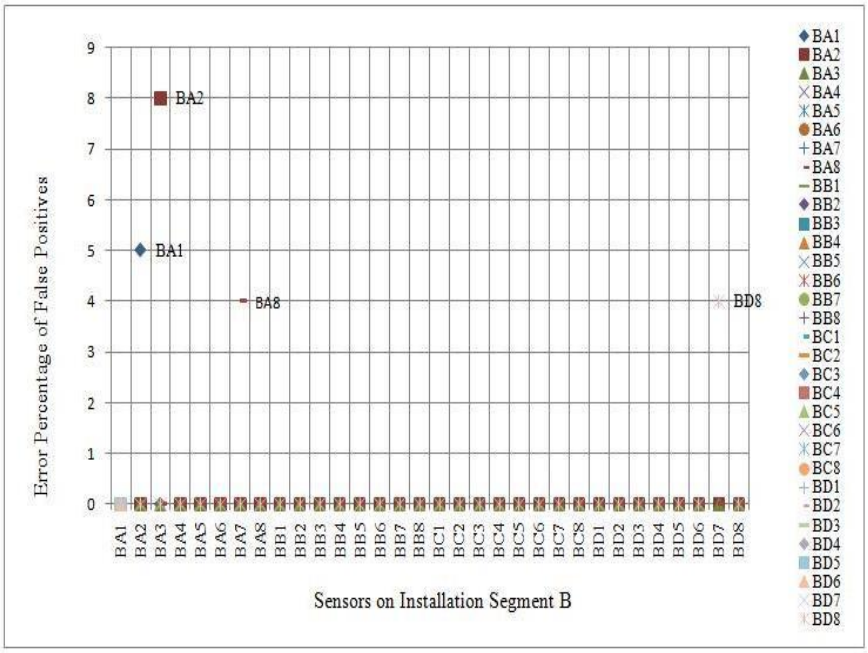

Figure 4.10: Figure displaying the error percentage of the false positives for the installation segment B. There were very few false positives observed. The maximum false positives were observed for sensor BA2 which was approximately 8%. The overall error rate was 0.65%.

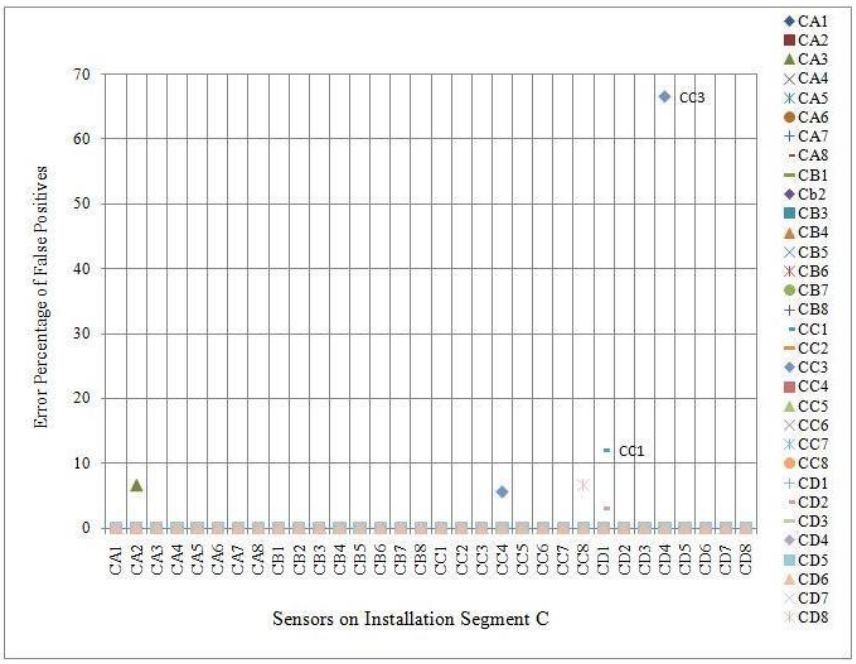

Figure 4.11: Figure displaying the error percentage of the false positives for the installation segment C. The maximum false negative error was obtained for sensor CD4 which is approximately 66%. The average error false positive rate for the 32 sensors was 0.098%.

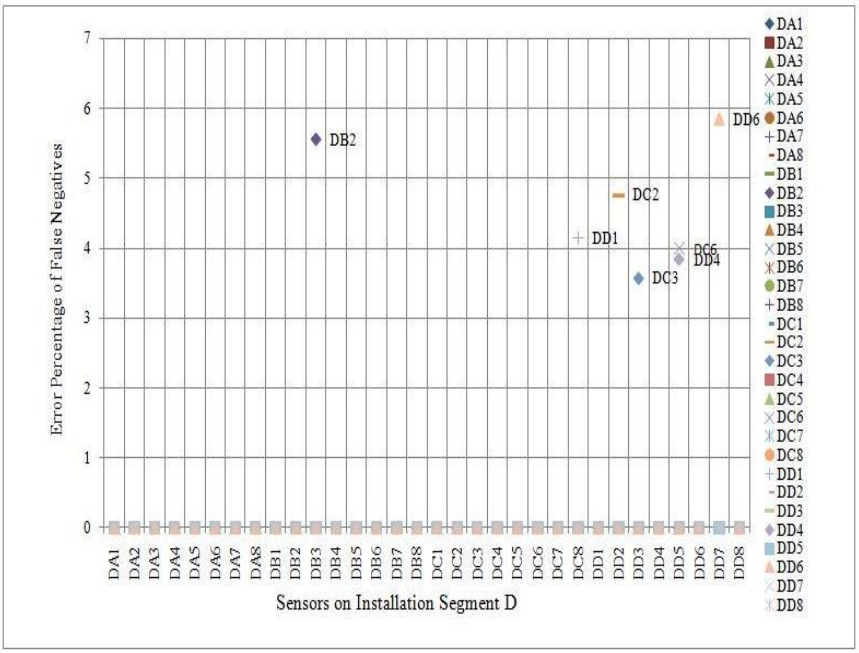

Figure 4.12: Figure displaying the error percentage of the false positives for the installation segment D. The maximum false negative error was obtained for sensor DD7 which is approximately 6%. The average false positives error rate observed for this segment was 0.03%.

The overall false positive rates observed for the installed floor were very less as compared to the development and the prototype systems. The highest error rate (66%) was obtained in installation segment C for sensor CD4. The average error rate for all the 128 sensors system was 0.0262%.

4.8 Amplifier Performance on the 4x8 Installation Segment and the Installed Floor.

The amplifier performance on both the 4x8 installation segment and the installed floor has been observed. It is found out that the response time for the micro-controller to select the 1 of the 32 sensors in the installation segment was 1ms. Thus, all the 128 sensors in the installed floor would be scanned in 128 ms.

Each Printed Circuit Board was powered using a single +5V power supply and was converted to +/-9V DC by NMH0509SC. A maximum current of 55.4mA was consumed by the complete circuit out of which a maximum of 43.2mA was consumed by 32 input buffers. The complete electronics setup was kept running overnight and it was observed that the performance was consistent and importantly repeatable. Spurious effects on the output of the amplifier unit were observed when the earth connection from the AC mains to the circuit ground was disconnected. Most prominent effect was the random generation of a series of HIGH output pulses from the amplifier unit without any excitation on the aluminum sensors.

CHAPTER 5: DISCUSSIONS

We have developed two faux floors using cheap and readily available components like wood and aluminum foil. We have additionally constructed a Smart Carpet, installed in a room and extensively tested it.

Aluminum foils serve the purpose of motion sensor with an advantage of not consuming any energy from a source. We regularly obtained a change of over 200% in the output amplitude of the aluminum foil sensor when they were activated. The values of these readings varied among the foil sensors. When the aluminum foil is activated, an increase in the stray electromagnetic field present in the aluminum foils causes a momentary rise in the output voltage.

Tests indicate that the size of the aluminum foils does affect their performance. We saw an almost linear rise in the output voltage with a non-linear rise in the area of the foil. The larger the aluminum foil, the stray electromagnetic energy radiated from the aluminum foil. Clearly we have electromagnetic noise since we saw that the sensors produced a higher output voltage when the lights are turned on. A higher output voltage is advantageous in our application as it meant higher sensitivity to even small perturbations in the atmosphere. Thus, the stray electromagnetic field, which usually is a cause of system upsets, can be vital for us in improving the efficiency of the system.

We designed and constructed a development faux floor to have an easily accessible and changeable means of trying out our ideas in the development of a personnel sensing system. This has been a very useful way to test each individual part of the system from the foil and its' attachment to wires to the display. It was important to set

up a system that is known to work then make the changes and observe improvements. The development board provides the capability to make changes in the electronic system and identify the best way to proceed.

Results obtained in Table 4-1 and Table 4-2 for the 7.6cm x 7.6cm sensor size indicates relatively high false negatives (misses) as compared to the other two sizes. This was an expected result as the possibility of a person's foot landing in empty space between two sensors was high causing a miss. It can be observed that the true positives and the false negatives always sum up to the total number of samples indicating that the true positives and the false negatives are complementary to each other. The deterioration in performance as we decrease to 7.6cm x 7.6cm aluminum foils, with the increased false negatives observed shows the impact of sensor size.

The results observed in the faux floor showed variability that we have identified sources of error in the construction of the faux floor. The performance data led us to observe a slight misalignment due to the drying of the wood that caused small but in some cases detectable errors on the other foils (16).

It is observed that the false negatives (miss) obtained for both the 15.2cm and the 30.5cm aluminum foils are extremely low, so the accuracy is very high. False negatives are important in our application since this can miss movements on the sensor floor. Lower values of misses indicate that the system is highly reliable as does high accuracy.

The effect of using a software filter (Table 4-5 and Table 4-7)Figure 4.5 showed tremendous results with an improvement of almost 13% in the system accuracy, 25% in the false positive rates (false alarms). The software filter had higher computations but instantly detected the foil activation. The reduction in the false positive rates with the

inclusion of filter would be extremely useful in systems which have high number of sensors (17).

In the prototype system, it was expected that increasing the number of sensors would produce an erroneous generation of stray signals and an increase in the cross talk between adjacent sensors resulting in false alarms. However, the number of adjacent sensors being falsely activated (false alarms) on the activation of only one sensor was very low indicated in Figure 4.7. The inclusion of software filter in the prototype system was an important factor enhancing the reliability of the prototype system. We observed that the prototype system was highly sensitive to small movements on the floor.

Major factors considered in determining the sensor for the installed carpet were its size, resolution and system reliability that would be achieved. The accuracy rate and the false positive rate results of 30.5cm x 30.5cm aluminum foils were the best among all the three sizes of sensors used in the development system. Comparing the performance of the 15.2cm and the 30.5cm aluminum sensors, we observed that the difference between their average accuracy is less than 2% and the difference in their average true positive rates was less than 3%. Using these observations and considering 50% sensor size reduction gave us confidence to design the installed floor with a 15.2cm x 15.2cm sensor size instead of a 30.5cm x 30.5cm sensor.

We performed the tests similar to the prototype system on the installed floor system. The number of pulses transmitted by the microcontroller on the activation of the sensors for 5seconds was recorded in the PC. Figures 4.8 to Figure 4.11 indicate we obtained a very low count on the false positives which indicated optimal system performance. The false positives followed a typical pattern. False positives were

observed in either adjacent rows or columns indicating the sensors were not accurately activated since the carpet was not marked for exact sensor location beneath it. Though the false positives obtained for sensor CD4 in segment C was high, the average false positive rate of the entire carpet was very low.

We determined the rate at which the activation on the sensors was successfully detected by the electronics unit. The scanning rate observed to be 128ms was fairly fast to detect the personnel movements. The 15.2cm spacing between adjacent sensors ensured a very low probability of the human foot placed within those 15.2cm and in turn increasing the accuracy. Thus, combined with higher accuracy, better resolution, smaller size of the sensors, and a high scan rate of the sensors, the installed carpet could be used for future developments and experiments.

We have found the appropriate characteristics of the amplifier to allow us to set up the floor in different environments. It is useful to repeat that we are detecting noise and there is considerable influence of the environment on the noise data that we acquire. The amplifiers designed for the faux floor system were three stage amplifiers and provided efficient signal conditioning of the sensor output. The op-amps used had extremely high slew rate to cope up with high data sampling rate of the sensor output. Though the opamp used was not a rail-rail opamp, its sensitivity and the voltage amplification was sufficient for the microcontroller to sense a HIGH input signal on its port. The output of the amplifier circuit seemed to die slowly when the sensor was activated as a result of inherited capacitance of the last op-amp that is interfaced with the microcontroller. The input impedance of the microcontroller when combined with the capacitance of the opamp creates a filter that results in the damping nature of the signal.

The 21 amplifier prototype board has an aluminum box containing all the electronics. This ensured portability of the entire system with a dual polarity power supply in place. Printed Circuit Boards were developed for the amplifier unit to minimize the noise due to wires, to accommodate a high density layout of components and have a cleaner solution for the analog circuitry.

The electronics design for the installed carpet had higher number of chips in it as a result of buffer stage for each sensor at the input. The inclusion of an input buffer stage was almost inevitable to achieve impedance transformation. However, the multiplexers definitely reduced the number of amplifiers which have feedback loops that cause a lag in signals. As a result, translation of signal from the sensors to the microcontrollers was almost instantaneous. A lot depended on how fast the analog multiplexers were switching the input channels to check activation on the inputs. With a scanning rate of 1ms/sensor, and a high slew rate of the op-amp (18V/usec), sensor activation was guaranteed detected. The entire analog circuit contained very few active elements, maintaining low power requirement. Each of the Printed Circuit Board had a maximum current capacity of 111mA, supplied by the NMH0509sc DC regulator.

An adapter with +5V output serving as power supply makes the circuit even more feasible to use in custom places. With a wireless microcontroller network built to gather and transmit the sensor data, the need of having a computer connected near to the installed carpet was ruled out (15). With the four Printed Circuit Boards packed in four boxes, attaching the complete electronics unit at a favorable position accomplished higher flexibility and portability.

CHAPTER 6: CONCLUSION

We have successfully built and demonstrated a floor covering which can detect movements of people on it. The developed system is extremely cheap and easy to manufacture. The results obtained from the aluminum foil acting as signal scavenging sensor has indeed been encouraging as the results are reproducible under nominal testing conditions. Inclusion of careful manufacturing including the ground plane in the sensor layout has proven to be very useful. The system is passive and detects presence of people. The faux floors provide us with a means to arrange foils on flat surface, activate the foils, and connect to the electronics sub-system which can be interchanged. The development system results were repeated in the higher versions of the systems we built.

There is a wide scope for improvement in the developed system for both the sensor floors and the electronics units. Identification of the optimal impedance for circuits leading from the sensors, refinement of the resolution of signals, using surface mount packages instead of DIP packages are some of the tasks that can be undertaken to improve system performance. Also, the use of low current, low power consuming op-amps can help in even more power management. The entire electronics package can be enclosed in a single box and could be indigenously powered up using simple low cost voltage adapter.

A comprehensive experimental technique to test the installed floor should be devised. There are several important variables that require consideration including environment such as humidity, temperature, floor type etc. The circuitry can be optimized to handle possible errors identified in each experiment, improving systems' robustness.

REFERENCES

1. CDC- Falls Among Adults: An Overview. *http://www.cdc.gov.* [Online] http://www.cdc.gov/homeandrecreationalsafety/falls/adultfalls.html.

2. M. Alwan, Rajendran, Prabhan Jade, Kell Steve, Mack David, Dalal Siddarth, Wolfe Matt, Felder, R., "A Smart and Passive Floor-Vibration Based Fall Detector for Elderly", In *Information and Communication Technologies,* 2006. *ICTTA*, 2006, Vol. 1, Issue 2, pp. 1003-1007.

3. Nevitt MC, Cummings SR, Hudes ES. Risk Factors for injurious falls: a prospective study. *J Gerontol* 1991; 46: M164 - 70.

4. Tyrer, Harry W., Neelgund, R., Mohammed, A., Shriniwar, U. (2009). Signal Scavenging for Passive Monitoring in Eldercare Technology, *Proceedings of the 31st Annual International Conference of the IEEE,* EMBS paper number 15901410: 6167 – 6170.

5. Domnic Savio, Thomas Ludwig, "Smart Carpet: A Footstep Tracking Interface," ainaw, *21st International Conference on Advanced Information Networking and Applications Workshops (AINAW'07)*, 2007 vol. 2, pp.754-760.

6. Koho Kalle, Suutala Jaakko, Seppanen Tapio and Roning Juha, "Footstep Identification from pressure signals using segmental Semi Markov models," in *Proceedings European Signal Processing Conference (EUSPICO),* 2004, 1609-1612.

7. Srinivasan P, Birchfield D, Qian G, Kidane A, "A Pressure Sensing Floor for Interactive Media Applications", *ACM International Conference Proceeding Series, Proceedings of the 2005 ACM SIGCHI International Conference on Advances in*

Computer Entertainment Technology, Valencia, Spain, ACM, 2005, Vol. 265, pp.278-281.

8. Caroline Rougier, Jean Meunier, Alain St-Arnaud, Jacqueline Rousseau, "Fall Detection from Human Shape and Motion History Using Video Surveillance," *21st International Conference on Advanced Information Networking and Applications Workshops* (AINAW'07), 2007 vol. 2, pp.875-880.

9. D. Anderson, R. H. Luke, J. M. Keller, M. Skubic, M. Rantz, M Aud, "Linguistic Summarization of Video for Fall Detection Using Voxel Person and Fuzzy Logic," *Computer Vision and Image Understanding, doi:10.1016/j.cviu*.2008.07.006, Vol. 113, pp. 80-89, 2008

10. Sixsmith A., Johnson N., Whatmore R., 2005. Pyrolitic IR sensor arrays for fall detection in the older population. *J.Phys. IV France*, vol. 128, pp. 153-160.

11. Popescu M., Li Y., Skubic M., Rantz M., 2008. An acoustic fall detector system that uses sound height information to reduce the false alarm rate. *IEEE EMBC08*, Vancouver, British Columbia, Canada, August 20-24, 2008, pp 4628-4631.

12. Koblasz, Arthur. Using RFID to prevent or detect falls, wandering, bed egress and medication errors. *US Patent 2007/0159332* A1 Atlanta, US, January 8, 2007.

13. Zhang, T., Wang, J., Liu, P., and Hou, J. Fall Detection by Embedding an Accelerometer in Cellphone and Using KFD Algorithm. *International Journal of Computer Science and Network Security*, vol. 6, issue 10, 2006.

14. Cosseddu P, Bonfiglio A, Neelgund R, Tyrer HW. Arrays of Pressure Sensors Based on Organic Field Effect : A New Perspective for Non Invasive Monitoring. *Conf Proc IEEE Eng Med Biol Soc. 2009*; 2009:6151-4.

15. Uday, Shriniwar. Data Control for a signal scavenging for personnel detection system. *Computer Engineering, University Of Missouri, Columbia. 2010*. Masters thesis for fulfilment of MS degree .

16. Harry W. Tyrer, Rohan Neelgund, Uday Shriniwar, KrishnaKishor D. Faux-Floor Development System for Personnel Detection Using Signal Scavenging Sensors.*32nd Annual International IEEE EMBS Conference, Argentina,* August 31-September 4, 2010 Under review.

17. Krishna Kishor, Devarakonda**.** Data display for a signal scavenging personnel detective system. *Computer Engineering, University of Missouri, Columbia* 2010. Masters thesis for fulfilment of MS Degree.

18. Capacitive Coupling – Wikipedia the free Encyclopedia found at [online] *http://en.wikipedia.org/wiki/Capacitive_coupling*

19. Capacitive Sensing - Wikipedia the free Encyclopedia found at [online] *http://en.wikipedia.org/wiki/Capacitive_sensing*

APPENDICIES

APPENDIX A – Data calculated but not utilized in the thesis

APPENDIX B – List of Electronics Components

APPENDIX C –Co-authored research papers

APPENDIX A – Data measured but not utilized in the thesis

A1. Data for development system with aluminum foil size 3in x 3in.

Date: 19 Feb 2010				
	Sensor A	Sensor B	Sensor C	Sensor D
COUNTS/50	false negatives for Sensor A	false negatives for Sensor B	false negatives for Sensor C	false negatives for Sensor D
false positives for Sensor A	15	0	0	0
false positives for Sensor B	0	5	0	0
false positives for Sensor C	0	0	4	0
false positives for Sensor D	0	0	0	5
Note:	this data is with filter			

Date: 20 Feb 2010				
	Sensor A	Sensor B	Sensor C	Sensor D
COUNTS/50	false negatives for Sensor A	false negatives for Sensor B	false negatives for Sensor C	false negatives for Sensor D
false positives for Sensor A	15	0	0	0
false positives for Sensor B	0	7	0	0
false positives for Sensor C	0	0	10	0
false positives for Sensor D	0	0	0	8
Note:	this data is with filter			

Date: 21 Feb 2010				
	Sensor A	Sensor B	Sensor C	Sensor D
COUNTS/50	false negatives for Sensor A	false negatives for Sensor B	false negatives for Sensor C	false negatives for Sensor D
false positives for Sensor A	9	3	0	0
false positives for Sensor B	0	2	0	0
false positives for Sensor C	0	0	1	0
false positives for Sensor D	0	0	0	5
Note:	this data is with filter			

A2. Data for development system with aluminum foil size 6in x 6in.

Date: 19 Feb 2010				
	Sensor A	Sensor B	Sensor C	Sensor D
COUNTS/50	false negatives for Sensor A	false negatives for Sensor B	false negatives for Sensor C	false negatives for Sensor D
false positives for Sensor A	5	0	0	0
false positives for Sensor B	0	7	1	0
false positives for Sensor C	0	0	3	0
false positives for Sensor D	0	0	0	3
Note:	this data is with filter			

Date: 20 Feb 2010				
	Sensor A	Sensor B	Sensor C	Sensor D
COUNTS/50	false negatives for Sensor A	false negatives for Sensor B	false negatives for Sensor C	false negatives for Sensor D
false positives for Sensor A	3	0	0	0
false positives for Sensor B	1	3	1	1
false positives for Sensor C	1	1	3	0
false positives for Sensor D	0	0	0	1
Note:	this data is with filter			

Date: 21 Feb 2010				
	Sensor A	Sensor B	Sensor C	Sensor D
COUNTS/50	false negatives for Sensor A	false negatives for Sensor B	false negatives for Sensor C	false negatives for Sensor D
false positives for Sensor A	7	0	0	0
false positives for Sensor B	0	3	0	0
false positives for Sensor C	0	0	5	0
false positives for Sensor D	0	0	0	15
Note:	this data is with filter			

A3. Data for development system with aluminum foil size 12in x 12in.

Date: 22 Feb 2010				
	Sensor A	Sensor B	Sensor C	Sensor D
COUNTS/50	false negatives for Sensor A	false negatives for Sensor B	false negatives for Sensor C	false negatives for Sensor D
false positives for Sensor A	1	1	0	0
false positives for Sensor B	0	4	0	2
false positives for Sensor C	0	0	4	0
false positives for Sensor D	0	0	0	3
Note:	**This data is with filter**			

Date: 22 Feb 2010				
	Sensor A	Sensor B	Sensor C	Sensor D
COUNTS/50	false negatives for Sensor A	false negatives for Sensor B	false negatives for Sensor C	false negatives for Sensor D
false positives for Sensor A	0	11	15	11
false positives for Sensor B	5	0	20	15
false positives for Sensor C	9	14	0	2
false positives for Sensor D	1	9	8	0
Note:	**This data is without filter**			

A4. Data of 12in x 12in with the effect of software filter.

Date: 23 Feb 2010				
	Sensor A	Sensor B	Sensor C	Sensor D
COUNTS/50	false negatives for Sensor A	false negatives for Sensor B	false negatives for Sensor C	false negatives for Sensor D
false positives for Sensor A	2	0	6	0
false positives for Sensor B	0	0	1	1
hfalse positives for Sensor C	0	0	0	0
false positives for Sensor D	0	0	0	3
Note:	**This data is with filter**			

Date: 23 Feb 2010				
	Sensor A	Sensor B	Sensor C	Sensor D
COUNTS/50	false negatives for Sensor A	false negatives for Sensor B	false negatives for Sensor C	false negatives for Sensor D
false positives for Sensor A	3	9	20	18
false positives for Sensor B	5	0	13	17
false positives for Sensor C	3	4	0	24
false positives for Sensor D	6	18	19	0
Note:	**This data is without filter**			

A5. Test data of the prototype system to determine its performance.

	A1	A2	A3	A4	A5	A6	A7	B1	B2	B3	B4	B5	B6	B7	C1	C2	C3	C4	C5	C6	C7
A1	1994	33	0	0	0	0	0	0	0	0	0	0	0	0	0	0	0	0	0	0	0
A2	0	905	0	0	0	0	0	0	0	0	0	0	0	0	0	0	0	0	0	0	0
A3	0	104	935	0	0	0	0	0	0	0	0	0	0	0	0	0	0	0	0	0	0
A4	0	0	0	1389	0	0	0	0	0	0	0	0	0	0	0	0	0	0	0	0	0
A5	0	0	0	0	1321	0	0	0	0	0	0	0	0	0	0	0	0	0	0	0	0
A6	0	0	0	0	0	1180	0	0	0	0	0	0	0	0	0	0	0	0	0	0	0
A7	0	0	0	0	0	52	1579	0	0	0	0	0	0	0	0	0	0	0	0	0	0
B1	0	0	0	0	0	0	0	1724	0	0	0	0	0	0	0	0	0	0	0	0	0
B2	0	0	0	0	0	0	0	0	1464	0	0	0	0	0	0	518	0	0	0	0	0
B3	0	0	0	0	0	0	0	0	0	1865	0	0	0	0	0	0	0	0	0	0	0
B4	0	0	0	0	0	0	0	0	0	0	1549	0	0	0	0	0	0	0	0	0	0
B5	0	0	0	0	0	0	0	0	0	0	0	1524	0	0	0	0	0	0	0	0	0
B6	0	0	0	0	0	0	0	0	0	0	0	0	1008	0	0	0	0	0	0	0	0
B7	0	0	0	0	0	0	0	0	0	0	0	0	73	1398	0	0	0	0	0	0	0
C1	0	0	0	0	0	0	0	0	0	0	0	0	0	0	1271	0	0	0	0	0	0
C2	0	0	0	0	0	0	0	0	0	0	0	0	0	0	0	1547	0	0	0	0	0
C3	0	0	0	0	0	0	0	0	0	0	0	0	0	0	0	0	984	0	0	0	0
C4	0	0	0	0	0	0	0	0	0	0	0	0	0	0	0	0	705	715	0	0	0
C5	0	0	0	0	0	0	0	0	0	0	0	0	0	0	0	0	0	35	815	0	0
C6	0	0	0	0	0	0	0	0	0	0	0	0	0	0	0	0	0	0	0	1665	0
C7	0	0	0	0	0	0	0	0	0	0	0	0	0	0	0	0	0	0	0	0	785

Figure A.1: Data sample 1 of the prototype system to determine its performance based on 5sec activation of the aluminum sensors.

	A1	A2	A3	A4	A5	A6	A7	B1	B2	B3	B4	B5	B6	B7	C1	C2	C3	C4	C5	C6	C7
A1	1762	0	0	0	0	0	0	0	0	0	0	0	0	0	0	37	0	0	0	0	0
A2	37	1107	0	0	0	0	0	0	0	0	0	0	0	0	0	0	0	0	0	0	0
A3	0	0	1630	0	0	0	0	0	0	0	0	0	0	0	0	0	0	0	0	0	0
A4	0	0	0	764	0	0	0	0	0	0	0	0	0	0	0	0	0	0	0	0	0
A5	0	0	0	0	974	0	0	0	0	0	0	0	0	0	0	0	0	0	0	0	0
A6	0	0	0	0	30	919	0	0	0	0	0	0	0	0	0	0	0	0	0	0	0
A7	0	0	0	0	0	0	1420	0	0	0	0	0	0	0	0	0	0	0	0	0	0
B1	0	0	0	0	0	0	0	1580	0	0	0	0	0	0	0	0	0	0	0	0	0
B2	0	0	0	0	0	0	0	0	1671	0	0	0	0	0	0	0	0	0	0	0	0
B3	0	0	0	0	0	0	0	0	0	2025	0	0	0	0	0	0	0	0	0	0	0
B4	0	0	0	0	0	0	0	0	0	0	1834	0	0	0	0	0	0	0	0	0	0
B5	0	0	0	0	0	0	0	0	0	0	0	2125	0	0	0	0	0	0	0	0	0
B6	0	0	0	0	0	0	0	0	0	0	0	0	716	0	0	0	0	0	0	0	0
B7	0	0	0	0	0	0	0	0	0	0	0	0	0	1841	0	0	0	0	0	0	0
C1	0	0	0	0	0	0	0	0	0	0	0	0	0	0	2060	0	0	0	0	0	0
C2	0	0	0	0	0	0	0	0	0	0	0	0	0	0	0	2106	0	0	0	0	0
C3	0	0	0	0	0	0	0	0	0	0	0	0	0	0	0	0	1455	0	0	0	0
C4	0	0	0	0	0	0	0	0	0	0	0	0	0	0	0	0	0	1081	0	0	0
C5	0	0	0	0	0	0	0	0	0	0	0	0	0	0	0	0	0	0	1873	0	0
C6	0	0	0	0	0	0	0	0	0	0	0	0	0	0	0	0	0	0	0	2073	0
C7	0	0	0	0	0	0	0	0	0	0	0	0	0	0	0	0	0	0	0	281	804

Figure A.2: Data sample 2 of the prototype system to determine its performance based on 5sec activation of the aluminum sensors.

	A1	A2	A3	A4	A5	A6	A7	B1	B2	B3	B4	B5	B6	B7	C1	C2	C3	C4	C5	C6	C7
A1	1674	0	0	0	0	0	0	0	0	0	0	0	0	0	0	0	0	0	0	0	0
A2	0	1224	0	0	0	0	0	0	0	0	0	0	0	0	0	0	0	0	0	0	0
A3	0	187	911	0	0	0	0	0	0	0	0	0	0	0	0	0	0	0	0	0	0
A4	0	0	0	489	0	0	0	0	0	0	0	0	0	0	0	0	0	0	0	0	0
A5	0	0	0	0	1523	0	0	0	0	0	0	0	0	0	0	0	0	0	0	0	0
A6	0	0	0	0	0	1397	0	0	0	0	0	0	0	0	0	0	0	0	0	0	0
A7	0	0	0	0	0	0	1747	0	0	0	0	0	0	0	0	0	0	0	0	0	0
B1	0	0	0	0	0	0	0	1989	0	0	0	0	0	0	0	105	0	0	0	0	0
B2	0	0	0	0	0	0	0	0	1118	0	0	0	0	0	0	0	0	0	0	0	0
B3	0	0	0	0	0	0	0	0	0	1329	0	0	0	0	0	0	0	0	0	0	0
B4	0	0	0	0	0	0	0	0	0	0	1298	0	0	0	0	0	0	0	0	0	0
B5	0	0	0	0	52	0	0	0	0	0	0	1937	0	0	0	0	0	0	0	0	0
B6	0	0	0	0	0	0	0	0	0	0	0	0	1174	0	0	0	0	0	0	0	0
B7	0	0	0	0	0	0	43	0	0	0	0	0	0	1539	0	0	0	0	0	0	121
C1	0	0	0	0	0	0	0	0	0	0	0	0	0	0	2172	0	0	0	0	0	0
C2	0	0	0	0	0	0	0	0	0	0	0	0	0	0	0	2039	0	0	0	0	0
C3	0	0	0	0	0	0	0	0	0	0	0	0	0	0	0	0	1638	0	0	0	0
C4	0	0	0	0	0	0	0	0	0	0	0	0	0	0	0	0	0	1174	0	0	0
C5	0	0	0	0	0	0	0	0	0	0	0	0	0	0	0	0	0	0	1673	0	0
C6	0	0	0	0	0	0	0	0	0	0	0	0	0	261	0	0	0	0	0	1386	0
C7	0	0	0	0	0	0	0	0	0	0	0	0	0	0	0	0	0	0	0	0	1935

FigureA.3: Data sample 3 of the prototype system to determine its performance based on 5sec activation of the aluminum sensors.

	A1	A2	A3	A4	A5	A6	A7	B1	B2	B3	B4	B5	B6	B7	C1	C2	C3	C4	C5	C6	C7
A1	98.727	0.6	0	0	0	0	0	0	0	0	0	0	0	0	0	0.6727	0	0	0	0	0
A2	1.1305	98.87	0	0	0	0	0	0	0	0	0	0	0	0	0	0	0	0	0	0	0
A3	0	7.725	92.275	0	0	0	0	0	0	0	0	0	0	0	0	0	0	0	0	0	0
A4	0	0	0	100	0	0	0	0	0	0	0	0	0	0	0	0	0	0	0	0	0
A5	0	0	0	0	100	0	0	0	0	0	0	0	0	0	0	0	0	0	0	0	0
A6	0	0	0	0	0.85082	99.149	0	0	0	0	0	0	0	0	0	0	0	0	0	0	0
A7	0	0	0	0	0	1.0838	98.916	0	0	0	0	0	0	0	0	0	0	0	0	0	0
B1	0	0	0	0	0	0	0	98.05484	0	0	0	0	0	0	0	1.9452	0	0	0	0	0
B2	0	0	0	0	0	0	0	0	89.14274	0	0	0	0	0	0	10.857	0	0	0	0	0
B3	0	0	0	0	0	0	0	0	0	100	0	0	0	0	0	0	0	0	0	0	0
B4	0	0	0	0	0	0	0	0	0	0	100	0	0	0	0	0	0	0	0	0	0
B5	0	0	0	0	0.92231	0	0	0	0	0	0	99.0777	0	0	0	0	0	0	0	0	0
B6	0	0	0	0	0	0	0	0	0	0	0	0	100	0	0	0	0	0	0	0	0
B7	0	0	0	0	0	0	0.8574	0	0	0	0	0	1.455633	95.2742	0	0	0	0	0	0	2.4128
C1	0	0	0	0	0	0	0	0	0	0	0	0	0	0	100	0	0	0	0	0	0
C2	0	0	0	0	0	0	0	0	0	0	0	0	0	0	0	100	0	0	0	0	0
C3	0	0	0	0	0	0	0	0	0	0	0	0	0	0	0	0	100	0	0	0	0
C4	0	0	0	0	0	0	0	0	0	0	0	0	0	0	0	0	19.184	80.816	0	0	0
C5	0	0	0	0	0	0	0	0	0	0	0	0	0	0	0	0	0	0.8545	99.1455	0	0
C6	0	0	0	0	0	0	0	0	0	0	0	0	0	4.8468	0	0	0	0	0	95.153	0
C7	0	0	0	0	0	0	0	0	0	0	0	0	0	0	0	0	0	0	0	7.385	92.615

Figure A.4: Diagonal elements represent the percentage of true positives obtained when the prototype system sensors were activated for 5sec. The other figures in the graph represent the false positives obtained during this test.

APPENDIX B – List of Electronics Components

B1. Pin Diagrams of the op-amp used.

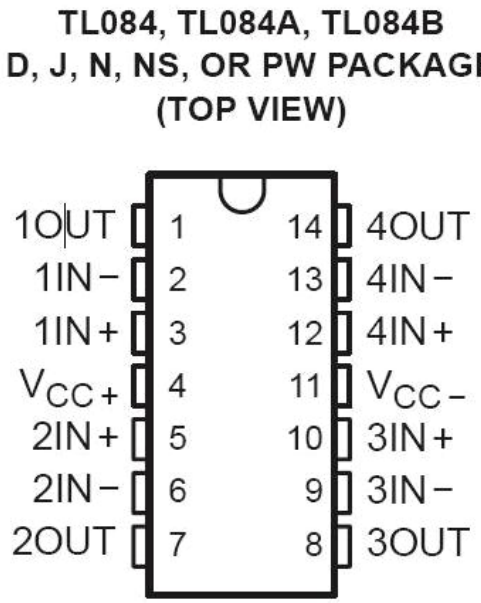

Figure B.1: Pin Diagram of TL084CN. This package contains four op-amps and has dual polarity.

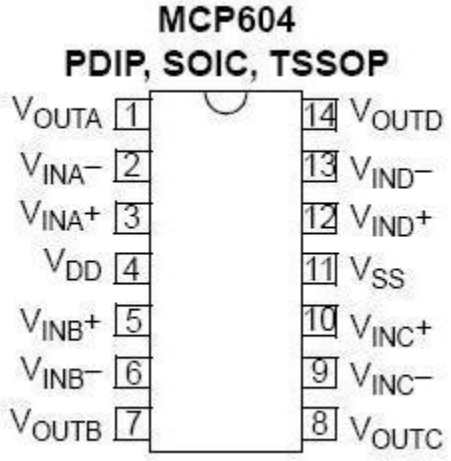

Figure B.2: Pin Diagram of TL084CN. This package contains four op-amps and has dual polarity.

B2. Parts list for the INSTALLATION SEGMENT (2010 prices)

Sr.No.	Component	Qty	Price (each)	Total
1	NMH0509sc DC-DC Converter	1	14.78	14.78
2	LM 7805	1	0.288	0.288
3	LM 78905	1	1.87	1.87
4	0.1uF Tantalum Cap 10%	4	0.321	1.284
5	1uF Tantalum Cap 10%	4	0.266	1.064
6	Resistor 30MΩ 5%	33	0.59	19.47
7	10nF Cap Ceramic 10%	33	0.052	1.716
8	TL084CN Op-Amp	1	0.346	0.346
9	MCP 604 Op-Amp	8	1.04	8.32
10	Resistor 2kΩ 1%	1	0.046	0.046
11	Resistor 10kΩ 1%	4	0.03	0.12
12	Resistor 1kΩ 1%	1	0.068	0.068
13	Resistor 20kΩ 1%	2	0.03	0.06
14	Resistor 100kΩ 1%	1	0.082	0.082
15	Diode 1N4148	2	0.016	0.032
16	CD4051 8:1 Multiplexer	4	0.754	3.016
17	CD4052 4:1 Multiplexer	1	0.754	0.754
18	8 pin Board to Board Connector	5	0.48	2.4
19	Connector Housing 8 pin	5	0.58	2.9
20	Crimp Socket Contact	20	0.04	0.8
21	DIP Socket 16 pin	5	1.05	5.25
22	DIP Socket 14 pin	9	1.31	11.79
23	Hook Up WIRE - red 100ft	1	11.39	11.39
		Total Price USD		**87.846**

APPENDIX C –Co-authored research papers

1. Signal Scavenging for Passive Monitoring in Eldercare Technology (presented at the 31st Annual International Conference of the IEEE Engineering in Medicine and Biology Society).
2. Arrays of pressure sensors based on organic field effect: A new perspective for non-invasive monitoring (presented at the 31st Annual International Conference of the IEEE Engineering in Medicine and Biology Society).
3. Inkjet Printed arrays of pressure sensors based on all-organic field effect transistors (will be presented at the 32nd Annual International Conference of the IEEE Engineering in Medicine and Biology Society).
4. Faux-Floor Development System for Personnel Detection Using Signal Scavenging Sensors (will be presented at the 32nd Annual International Conference of the IEEE Engineering in Medicine and Biology Society).

Signal Scavenging For Passive Monitoring In Eldercare Technology

Harry W. Tyrer *Member, IEEE*, Rohan Neelgund, Ashrafuddin Mohammed, Uday Shriniwar

***Abstract*—Signal scavenging is analogous to energy scavenging: seemingly ubiquitous energy in the environs provides the signal for usage as a personnel sensor. Such energy can be used to detect motion, and most importantly falls. Stray signals can be detected in aluminum foil as voltage differences between touched foil (say by hand) compared to that untouched. Spectrum analysis shows the stray electromagnetic noise signal consists substantially of 60 Hz and its harmonics. Also the signal intensity for both touched and untouched monotonically increases with foil area. While personnel monitors find utility in many areas including security, personnel control and activity detection, we believe these putative sensors to be useful in inobtrusive monitoring of elders to provide them with increased independence at a critical time in their lives.**

I. Introduction

Energy scavenging recognizes that energy exists in the environment in a wide array of forms. A common example is the self winding watch that uses wrist motion to provide energy for operation. Other common examples include the use of solar, wind and ocean energy; these sources can and do provide large amounts of energy, as is well known.

The sensor engineer is familiar with the nuisance of 60 Hz and other stray electromagnetic noise that limits the operation of the sensor, and may even require extensive effort to overcome. We propose using this noise as a ubiquitous source of signal. We use the term signal scavenging to describe the use of that noise as a source of energy for signal detection. In particular we are interested in using the fact that the noise level read from a sample of aluminum foil increases when touched by a person.

The motivation for this study is to use signal scavenging as a means to monitor the elderly for motion and falls. There are many applications for unobtrusively monitoring the elderly [1]. Inobtrusive means the individual has given their explicit permission for this monitoring and aware if it, the individual need take no action to effect the operation or performance of the system and the individual's privacy is not violated. Studies in our group indicate that older adults were concerned about falls and that they perceived technologies that monitor activity levels and sleep patterns as useful. The older adults emphasized the need for non-obtrusive systems [2]. A monitoring system using these foils is passive and will increase the effectiveness of caregivers by providing access to the motion of the individual.

The elderly are particularly vulnerable to falls. Falls are dangerous and require immediate assistance; there are anecdotes of those who have fallen and waited undiscovered for hours or even a day or more. In addition, predilection to conditions such as falls, and changes in daily patterns may indicate impending health problems [3]. Inobtrusive sensing technology can provide alerts. More generally, there is evidence that technology can provide early detection of changes in the health status of the elderly [4], and we believe that a monitoring system with careful attention to the data can provide those benefits.

Monitoring and fall detection is also important for those with Alzheimer's, since it has been known for a while that falls also are associated with cognitive dysfunction [5]. Some of the published literature indicates that approximately 60% of older people with cognitive impairment fall annually, that's approximately twice that of older people without cognitive impairment. The increased odds of falling in older adults with cognitive impairment put them at increased risk for major injury such as fracture and head trauma [6]. A more recent study shows that women with mild cognitive impairment have a greater number of fall risk factors compared to older women without mild cognitive impairment [7], and these women had significantly reduced balance and limb coordination.

In this paper we characterize the signal scavenged from aluminum foil for the purpose of developing an inobtrusive sensor system for the elderly. We characterize the voltages detected upon activating (touching) the foil and non-activating. We further characterize the noise by the low frequency spectra appearance the dependence of the detected voltage on foil area.

II. Methods

We undertook a series of experiments to identify the properties of the noise signals that we read from aluminum foils. For these experiments we used Hewlett Packard 54602B laboratory oscilloscope, with 150 MHz bandwidth, two channels and millivolt sensitivity. A Tektronix 4 Channel Oscilloscope (TDS3054B) was used for the spectrum analysis.

Manuscript received April 19, 2009. This work was supported in part by the Alzheimer's Association ETAC grant program. The authors are with the Department of Electrical and Computer Engineering at the University of Missouri – Columbia, Columbia, Missouri 65211, USA. Harry W. Tyrer is the corresponding author with telephone number 573 882 6489 email tyrerh@missouri.edu.

The foils were laid out and connected to the oscilloscope through wires glued to the foil using MCG-8331 MG Chemicals Silver Conductive Epoxy. The glue has high electrical conductivity, although no direct measures of conductivity were made. Figure 1 shows a typical square sample of aluminum foil with glued wires (which connect to the oscilloscope).

Figure 1 Aluminum foil covered by vinyl (for protection and ease of use) with leads glued in place.

We measured electrical energy from foils with and without contact with a person. We refer to activated foils as those touched or in contact with a person. In case of comparisons the contact was applied the same way. In many experiments we stepped on the foil and read the activation, in others we touched by hand, and still others it was most convenient to apply hand pressure on the foil covered with transparent sheet of plastic. Non-activated, inactivated, or non touch foil data was read without touching or stepping on the foil.

III. Results

We compare a single measure of activated and non-activated foil in the plot shown in figure 2. The activated signal level is at hundreds of millivolts compared to the non-activated, at 10s of millivolts. As will be shown and discussed below we also measured the activated and non-activated average voltages of 10.77 mv and 2.33 mv, and the RMS voltages at 53.99 mv and 5.25 mv. These comparisons help characterize the voltages indicating that there is not much of DC component. Secondly, variations in the 'scope display due to variations in touching can produce noticeable differences in the various voltage readings indicating a temporary variation in DC component.

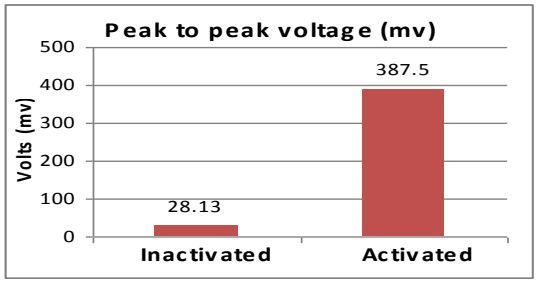

Figure 2 shows the peak to peak voltage read when the foil is momentarily touched.

The foil acts as an antenna that when touched acquires a substantial increase in ambient electrical energy. The oscilloscope shows (Fig 3) the signal variation with and without activation. To obtain reasonably repeatable result we touched the foil in similar ways each time. The manner of touching produced different wave forms in comparing differences between activated and non-activated. Clearly a motivation of this study is to learn to tame the signal source.

Figure 3 Electrical energy added to the foil as a result of a person touching (activating) the foil. The smaller noisy portion of the trace has a level at 30mv p-p, whereas the larger activated potion is nearly half a volt.

We prove here that this electrical energy consists of stray electromagnetic energy ubiquitously available in the environment. The sources include 60 Hz power line energy, stray energy from nearby electrical or electronic equipment or appliances, radio and television station signals, and possibly other sources including wireless Personal Digital Devices. To try to identify these sources we decided to obtain the spectrum of the signal. It was most confinement to focus on the low frequency (2.5 kHz and lower) energy.

We obtained data from activated (touch) and non-activated (non-touch) foils. The data was downloaded onto an excel spread sheet and the plots shown here.

We obtained a linear display of the spectrum from dc to 1500 Hz. Shown in figure 4 is a linear display of signals obtained from non activated foil. The 60 Hz is the dominant component in this display (see table 1).

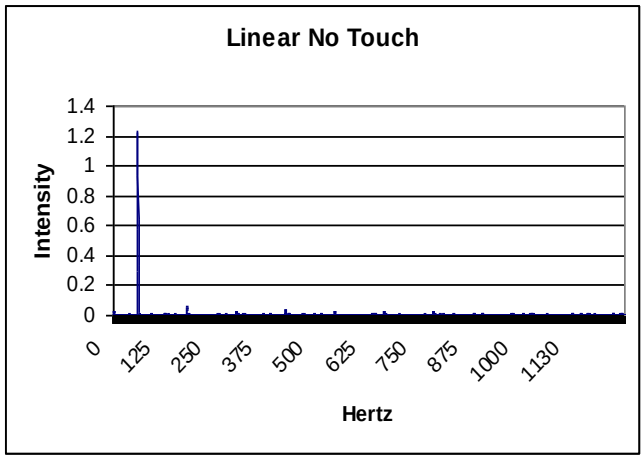

Figure 4. Display of the linear spectrum of data acquired from a foil of aluminum connected to an oscilloscope. Note the substantial spike at 60 Hz.

It is the most easily identifiable component of the data and includes the 60 Hz signal and its frequency components or harmonics.

The same data was displayed in logarithmic mode to diminish the 60 Hz component and enhance the other prominent components (Figure 5) Note the spikes of

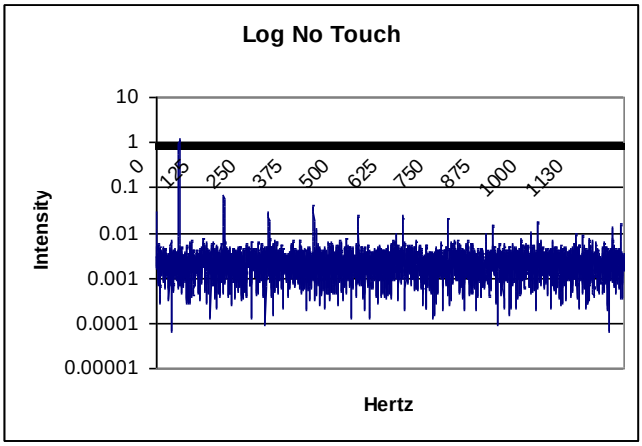

Figure 5 allows a reading of the components expressed in table 2.

components of odd harmonics of 60 Hz, and note the substantial noise levels between the spikes; these remain to be studied. Table 1 lists the frequencies and amplitudes directly read from figure 4. Beyond 900 Hz it is difficult to honestly discriminate the level of the 60 Hz components since they are approaching the level of other data spikes not readily attributable to 60 Hz components.

Table 1 Amplitude and frequency of prominence in the noise energy.

Frequency	Amplitude
60	1.226
180	0.066
300	0.029
420	0.018
540	0.022
660	0.024
780	0.021
900	0.015

The most remarkable fact here is that these are the odd harmonics of 60 Hz (1, 3, 5…). We looked carefully at the time domain signal for this spectrum, which was triangular, with 60 pulses/sec repetition rate. Riding on top of the triangular patter were small components of amplitude variation. Providing confirmation that we indeed were dealing with odd harmonics of 60 Hz

We obtained the spectrum of the noise data from 6inch square aluminum foil. We compare the activated (touched) foil to inactivated foil (no touch) to form figure 6. We see that the 60 Hz component spikes were consistently larger in the touch case compared to the no touch case. Remarkable we also see even harmonics of 60 Hz, which were suppressed in figures 4 and 5 above, indicating the statistical nature of the noise. In this case the even harmonics are substantially reduced compared to the nearest odd harmonic. Furthermore in the activated (touch) case the drop in amplitude is more pronounced than that of the inactivated case.

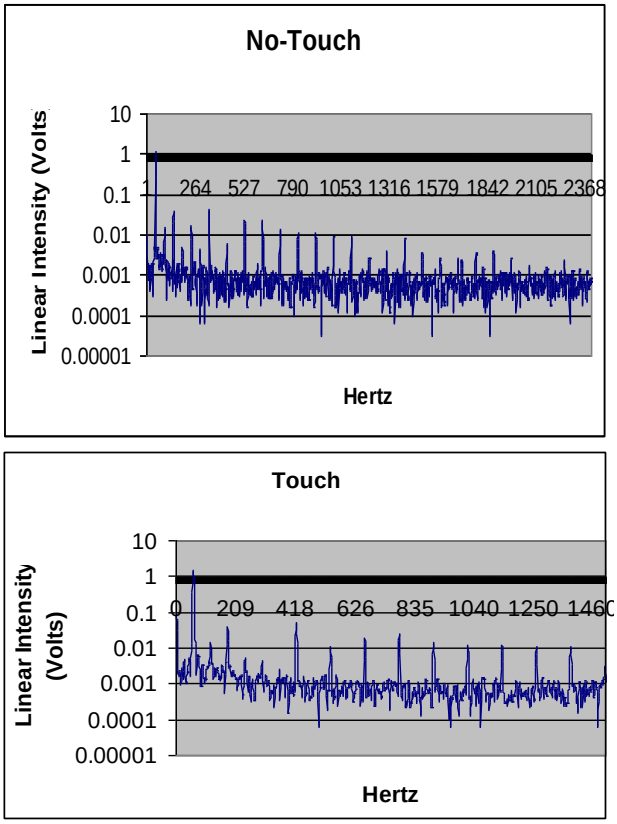

Figure 6 (upper) the log of voltage intensity for activated foil samples. Note the predominance of the odd harmonic, but the even harmonics are distinct from the background. (Lower) The inactivated foil shows a substantially lower harmonics compared to the activated foil.

It has come as a surprise to us that there does not appear too much randomness in these data. This clearly needs substantially more study. But the primary source of energy clearly comes from 60 Hz stray signals. We are so accustomed to calling noise and stray signals random, that it is surprising that the easy call of random signal cannot be yet be affirmed or denied.

Clearly for use as sensors it is important to consider the variation in size. We obtained the touch and no touch values of noise from 6 foils ranging in area from 2, 4, to 64 square inches and plot the results in Figure 7. There is clearly a separation between the activated and non-activated values. We should point out that similar data was obtained for peak to peak voltage (112 mv inactivated, and 900 mv activated). Interestingly the size of the foil is important since

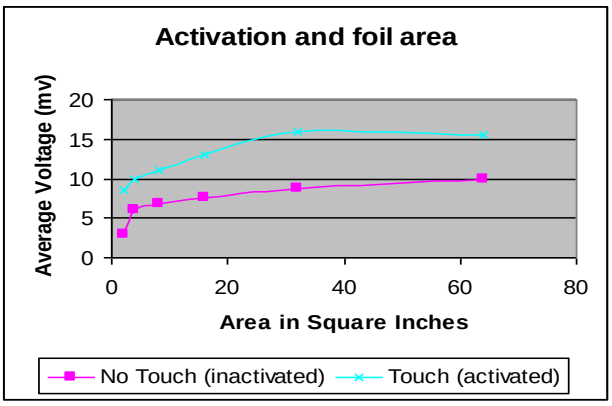

Figure 7 Comparison of activated and non-activated foils by size. The voltage monotonically increases with a linear increase in area. Here we compare the average voltage. At the smaller sizes we risked losing the signal altogether, with increasing area we reach an inflection point at around 32 sq. in. Further increase in size does not improve the signal difference.

larger provides more signal. But smaller provides more resolution. We note the maximal inflection of the activated data at 32 sq in. This point seems to be that at which the method of touch that we used did not increase the noise level appreciably, a trend the non-activated foils did not express. The foils were strips 4 inches long with the appropriate width to fill out the required area (the last though was 8" x 8"). This gives the intriguing possibility of providing improved resolution compared to the larger foils.

IV. Discussion

Signal scavenging takes advantage of stray electromagnetic energy to detect the presence of (or the touching by) personnel in a conductive foil. We used aluminum foil which is cheap and easily available. This is similar to the capacitive buttons used in electronic systems except that we do not use any energy source other than that picked up by the foil. This of course is the chief advantage in that there is no need to provide power and the foils are completely static devices.

Clearly the primary source of energy is 60 Hz stray electromagnetic energy. Furthermore the activated foils show a substantial increase in the main 60 Hz signal, which is 20 to 40 times greater than the higher harmonics of the waveform. Additionally there is some variation in the detected signal where we have seen primarily odd harmonics and other times we see both odd and reduced even harmonics. While this is an interesting insight, it does not really affect the detection of the noise since we use total noise. We continue to explore ways of improving the detection of the signal. There is some satisfaction in using as a signal source the stray energy that is the bane of most sensor engineers, namely the 60 Hz stray noise.

We have been concerned about repeatability and reliability. Are there places where this system will not work? Clearly in Europe where 50 Hz power is used, we should see those frequencies in our data; again this is not a problem for the same reason that amplitude discrepancies at various 60Hz components do not trouble us. However in those locales where no electrical energy is present or where it is far away we may not have sufficient stray noise to detect.

V. Conclusion

We have shown that it is possible to use passive foils to distinguish between activated and non-activated foils; activation means touching. We have provided low frequency characterization of the scavenged signal to be 60 Hz stray electromagnetic energy with the first 10 harmonic components providing recognizable increases in energy. Furthermore the signal strength, as expected, monotonically increases with foil area.

Future work will be to further characterize the scavenged signal and to develop sensors.

VI. Acknowledgment

We gratefully acknowledge funding for this project from the American Alzheimer's Association under the ETAC program. The authors thank Jim Fischer for his help in obtaining access to the spectrum analyzers and for discussion on these findings.

References

[1] Tyrer, H., Alwan, M., Demiris, G., He, Z., Keller, J., Skubic, M., Rantz, M., "Technology for Successful Aging", *Proceedings, IEEE 2006 International Conference of the Engineering in Medicine and Biology Society*, New York, NY, August 30-September 3, 2006, pp. 3290-3293.

[2] Demiris, G., Rantz, M.J., Aud, M.A., Marek, K.D., Tyrer, H.W., Skubic, M., & Hussam,A.A. (2004). Older adults' attitudes towards and perceptions of "smart house" technologies. *Medical Informatics and the Internet in Medicine, 29*(2), 87–94.

[3] Rantz MJ, Porter R, Cheshier D, Otto D, Servey CH, Johnson RA, Skubic M, **Tyrer H**, He Z, Demiris G, Lee J, Alexander G, & Taylor G TigerPlace, a State-Academic-Private Project to Revolutionize Traditional Long Term Care, *Journal of Housing for the Elderly*, *22*(1/2), 66-85, 2008

[4] **Tyrer HW**, Aud MA, Alexander G, Skubic M, Rantz M. Early Detection of Health Changes in Older Adults, *Proc., IEEE 2007 Intl. Conf. of the Engineering in Medicine and Biology Society*, Lyon, France August, 2007, pp. 4045-4048.

[5] Tinetti ME, Speechley M, Ginter SF. Risk factors for falls among elderly persons living in the community. *N Engl J Med*. 1988;319:1701–1707

[6] Van Dijk PT, Meulenberg OG, van de Sande HJ, et al. Falls in dementia patients. *Gerontologist*. 1993;33:200–204

[7] Liu-Ambrose T, Ashe, M.C, Graf P, Beattie, B.L. and Khan, K.M. Increased Risk of Falling in Older Community-Dwelling Women With Mild Cognitive Impairment Phys Ther Vol. 88, No. 12,1482-1491,2008

Arrays of pressure sensors based on organic field effect: a new perspective for non invasive monitoring

Piero Cosseddu, Annalisa Bonfiglio, Rohan Neelgund, Harry W. Tyrer, *Member, IEEE*

Abstract— In this paper we propose totally flexible organic field effect transistors (OFETs) assembled on plastic films as sensors for mechanical variables. In the first part, mechanical sensors for pressure and bending detection are presented. A sharp and reversible sensitivity of the output current of the device to an elastic deformation induced by means of a mechanical stimulus on the device channel has been observed and suggested the idea of employing arrays of such sensors for detecting the deformation applied onto a planar surface. In the second part, the possibility of using similar devices for bio- and chemo-detection is described. By exploiting the properties of the basic structure, the device can be combined with any kind of substrate to detect for instance the pressure applied by people walking or standing on a functionalized carpet. This emerging technology seems to be promising for applications in the field of remote and non invasive monitoring of elderly and disabled people.

I. Introduction

Research in biomedicine and engineering during the last years has led to a remarkable interest in sensor technologies for biomedical applications. Silicon technology is not suitable for manufacturing low-cost large-area sensor devices that are preferably light, flexible, and even disposable (for some biomedical applications). Its inherent high temperature fabrication processes make it very difficult to use inexpensive flexible substrate materials, resulting in high fabrication costs. On the other hand, organic semiconductor-based devices offer very interesting opportunities for sensor applications due to the low-cost and easy fabrication techniques, and the possibility of realizing devices on large and flexible areas on unusual substrates as paper, plastic or fabrics. Sensors seem therefore to be the optimal candidate for fully profiting from the properties of organic materials. Organic materials, based on conjugated organic small molecules and polymers, have paved the way, in the last decade, for the production of devices on large-area, low-cost, plastic substrates.

Manuscript received April 19, 2009. This work was supported in part by the Alzheimer's Association ETAC grant program. P.C. and A.B. are with the University of Cagliari Department of Electric and Electronic Engineering, Piazza d'Armi 09123 Cagliari, Italy and with INFM-S3 "nanoStructures and bioSystems at Surfaces", Modena, Italy. H.W.T. and R.N are with Department of Electrical and Computer Engineering, University of Missouri – Columbia, Columbia, Missouri 65211. Harry W. Tyrer is the corresponding author with telephone number 573 882 6489 email tyrerh@missouri.edu.

So far, great progress has been made in the field of optoelectronic devices, like Organic Light-Emitting Diodes (OLEDs) [1] and for switching functions by means of Organic Field Effect Transistors (OFETs) [2].

Organic semiconductors offer several advantages due to easy processing, good compatibility with a wide variety of substrates including flexible plastics, and great opportunities in terms of structural modifications. Furthermore, thin films of organic semiconductors are mechanically robust and flexible, and this characteristic offers interesting possibilities for future electronic/sensor applications based on flexible substrates.

In this paper, we report on arrays of organic field-effect transistors that have been employed for pressure detection on relatively large surfaces. Despite the low mobility of organic materials (compared to crystalline semiconductors, it is about three orders of magnitude lower [3]) there are applications, as the recently suggested electronic skin [4], in which the lower speed is tolerable and the use of organic materials seems to be more beneficial than detrimental. In fact, being able to obtain large sensing areas is certainly a benefit for a wide set of applications and using printing techniques for creating sensing devices on unusual substrates could certainly widen the set of possible applications where sensing is required.

Relatively little progress has been made in the field of pressure or bending recognition [5]-[7] compared to the areas of gas [8] and chemical sensing [9], mainly because mechanical sensing requires attributes of conformability and flexibility and three-dimensional large area shaping that in many cases are difficult to achieve even for organic devices.

The effect of strain on the mechanical and electronic properties of organic semiconductors is an emerging research topic in fundamental physics and applications. Although mechanical flexibility is one of the main advantages of organic materials, organic semiconductors strain properties have not yet been fully exploited in order to realize devices for detecting physical parameters as for instance pressure or bending.

II. Experimental

We recently proposed an innovative, substrate-free, organic field-effect transistor structure based on

pentacene for pressure and strain detection [10]. A cross section of the structure is shown in Fig. 1.

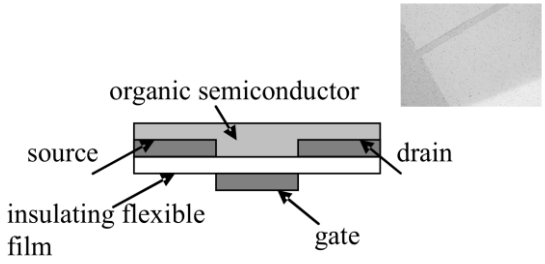

Fig. 1. Cross section of substrate-free OFET for sensing applications. Inset: detail of the device channel.

The main peculiarity of this structure is that it is assembled starting from a flexible insulating film, but without any substrate. Thanks to this feature, both sides of the insulating layer are accessible so it is possible to apply to both of them an external stimulus (i.e. a pressure) or to glue the final flexible device onto whatever kind of substrate (for instance a 3-D surface). This is usually impossible for structures assembled on a rigid substrate as, typically, OFETs realized on Silicon/Silicon dioxide, in which the presence of the substrate drastically limits the flexibility of the device. The flexible insulating layer is a thin polyethylene terephthalate sheet Mylar^{TM}, Dupont, with thickness 1.6 µm, dielectric constant 3.3, dielectric rigidity of 10^5 V/cm that allows to apply a gate bias sufficiently high to induce a field-effect in the organic semiconductor.

Thanks to its electrical and chemical characteristics, Mylar can be used as received without any further surface treatment while thanks to its mechanical properties it acts not only as gate insulator but also as mechanical support for the whole structure. This is usually impossible with conventional organic dielectrics that are solution-processed; in this case, as a matter of fact, a flattening support is essential. To form a transistor structure, gold bottom-contact source and drain electrodes were patterned on the upper side of the flexible dielectric foil, using a standard photolithographic technique, while the gold gate electrode lied on the opposite side. The channel width (W) and length (L) used were 5 mm and 150 µm respectively, in an interdigitated configuration. Since the Mylar is transparent to UV light, in the photolithographic process for the device assembly, source and drain may be used as mask for the gate patterning. This point is a distinctive feature of our structures and it is a consequence of the absence of the substrate. As a consequence of the auto-alignment between source-drain and gate electrodes, all the parasitic capacitance effects due to metal overlapping are drastically limited [10]. A 50 nm thick vacuum-sublimed Pentacene (Sigma-Aldrich) is used as active layer. Arrays of such devices have been produced on Mylar films, realizing 3x3 matrix structures as shown in Fig.2.

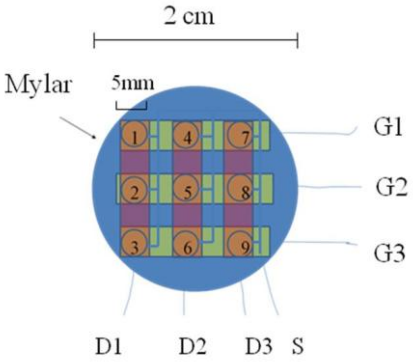

Fig. 2. Schematic representation of the employed matrix configuration

As can be noticed, a common source configuration was used, where, all the devices in the same row have a common gate and all the devices in the same column have a common drain. In this way every single transistor in the matrix can be switched on independently. In this way, a spatial resolution of c.a. 9 devices over 4cm^2 area was achieved, with 25mm^2 area per each device and a lateral spacing of 2mm between two adjacent devices.

III. Results

All the assembled devices within the active matrix showed typical p-type field effect behaviour with reproducible electrical performances. In particular, p-type OFETs with hole mobilities up to 10^{-1} cm^2/Vs and I_{on}/I_{off} up to 10^5 were obtained.

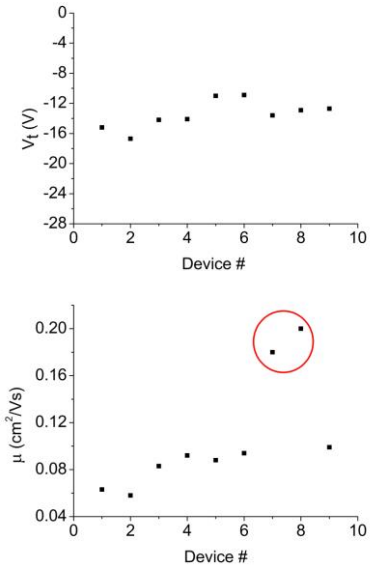

Fig. 3. An example of the electrical performances of all devices within the matrix.

Moreover, as can be seen from the graphs reported in Fig. 3, the devices are characterized by a very similar electrical behaviour with a very uniform threshold voltage, close to -15V. Also, a rather similar mobility was found; only 2 within 9 devices gave rise to a mobility value which is not comparable to the other samples. This is very important, because it shows that even a non conventional substrate, not optimized for organic electronics applications, can be employed for the realization of high performances OFETs. These matrixes of distributed sensors were employed for pressure detection. In order to avoid the active layer degradation during the experiments, a thin (1 mm thick) polydimethylsiloxane (PDMS) film was deposited on the entire surface of the matrix. The electrical response of a certain device within the matrix was then monitored when an external pressure is applied to every single transistor area separately.

In this example, reported in Fig. 4 where the electrical behaviour of device #1 is shown, the device has been biased using V_{DS}=-10V and V_{GS}=-10V. As can be clearly seen, despite very small applied pressures, approximately 1kPa (around 3g/0.25cm^2), the device showed a marked decrease of the measured current when the external stimulus is applied; moreover, a significant response has been observed only when pressure was applied on its own surface area.

It is noteworthy, that even if the lateral spacing between two adjacent transistors is rather small (around 2 mm), no significant current variation has been measured when pressure was applied to the adjacent cells within the same row. When pressure was applied on adjacent transistors in the same column, meaning that the two devices (the mechanical stressed and the measured one) have the same source and drain electrodes, as can be noticed in Fig. 4, a very slight change in the monitored device current can be measured, which can be possibly be attributed by electrical interference introduced by the mechanical deformation of source and drain electrodes which, in this case, have the same potential of the monitored device one. However, it can be also observed that such a change in the current is much smaller (ranging around 2%) than the one measured when the pressure was applied directly on the same device.

In synthesis, we developed a fully flexible matrix of distributed transistors which can be used for monitoring mechanical deformation (in this case induced by an external pressure applied to the single devices). The described system showed very good reproducibility of the results and very good spatial resolution, with 0.25cm^2 sensors with vertical and horizontal spacing of 2mm. As a result, this system can be used for monitoring pressure distribution over large areas with very good spatial resolution. Moreover, thanks to the very high flexibility

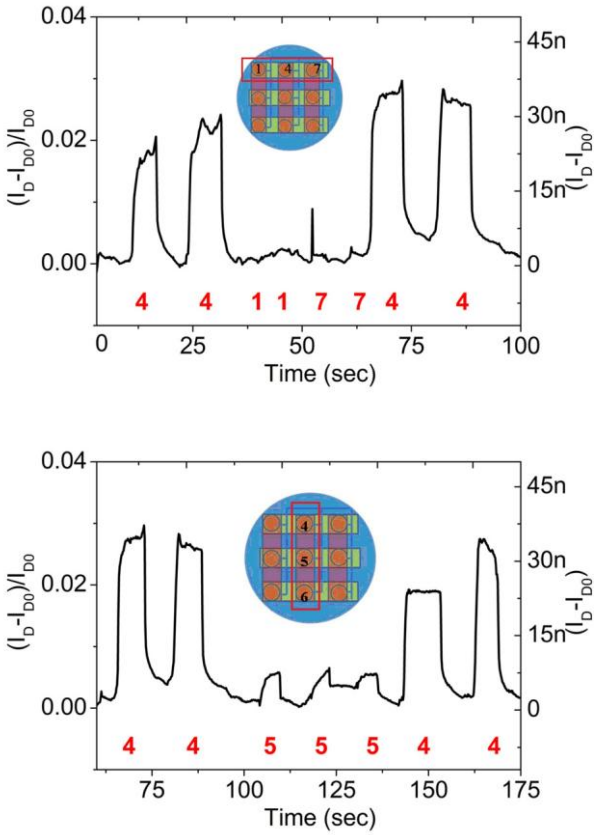

Fig. 4. Drain current variation recorded in device #1 when pressure was applied to adjacent devices in the same row (a), in the same column (b). The red numbers reported in the bottom of the plot indicate on which device the pressure is applied.

of the employed structure, such a system can be very easily transferred onto whatever kind of substrates, as paper, fabric or 3D structures allowing a very wide range of possible applications.

IV. Applications: A Smart Carpet for Remote Monitoring

An important bio-engineering application uses these area detectors to monitor the elderly and even to provide security. Detecting the walking pressure or the individual prone on the floor can provide a rapid means to alert care givers to respond to falls. Falls are a leading cause of death of the elderly. In security the area sensor detects footfalls on a location where there should be none or where there is corroborating indication of unauthorized entry.

The signal requires connecting the sensor to an amplifier then a microprocessor and to a computer. This provides ample capability to determine which sensors send the data and to display it in some meaningful way- e.g. a map of the floor. The variables that allow for choice of sensor include the power supply, the geometric arrangement of the arrays and the signal detection matrix. For example one configuration is to set the power supply lines fixed

and to obtain row and column data from FET source. Such an arrangement avoids the mxn detection and allows for m+n data lines. An important issue is the low level of current that must be amplified; furthermore the high impedances allow for low currents.

Finally future work will be to test these in a patient's room. In the immediate future we will test mock up carpets to determine the best placement of sensor and carpet so that there is no slippage or cushioning. Individuals with dementia expend significantly more effort in walking than those with out cognitive challenges.

V. CONCLUSIONS

In conclusion, we have presented a system for pressure detection on relatively large areas based on the use of organic thin film transistors for realizing arrays of pressure sensing units on planar plastic surfaces.

These results are very promising in view of innovative applications in the field of remote and non invasive monitoring of elderly and disabled people. In particular, the realization of distributed transistors and sensors by printing techniques is the most promising perspective for this kind of applications as it would allow producing large areas with a very fast method.

ACKNOWLEDGMENT

The American Alzheimer's Association is gratefully acknowledged for funding the project under the ETAC Program. The European Commission is gratefully acknowledged for funding the project under the Programme IST-IP, VI FP Project n. 26987, PROETEX.

REFERENCES

[1] [1]. T. Tsujimura, SID 2003 Technical Digest Vol.XXXIV, Book 1,6 (2003).

[2] [2] C. Dimitrakopoulos, P. R. L. Malenfant, Adv. Mater. **14**, 99 (2002).

[3] [3] B. Crone, A. Dodabalapur, Y-Y. Lin, R.W. Filas, Z. Bao, A. LaDuca, R. Sarpershkar, H.E. katz, W. Li, Nature 403, 521, 2000

[4] [4] T. Someya, Y. Kato, T. Sekitani, S. Iba, Y. Noguchi, Y. Murase, H. Kawaguchi, T. Sakurai, PNAS 102, 35, 2005

[5] [5] T. Someya, T. Sakitani, S. Iba, Y. Kato, H. Kawaguchi, T. Sakurai, PNAS 101, 27, 2004

[6] [6] G.Darlinski, U. Böttger, R. Waser, H. Klauk, M. Halik, U. Zschieschang, Günter Schmid, C. Dehm, Appl. Phys. Lett. 97, 093708, 2005

[7] [7] T. Sekitani, Y. Kato, S. Iba, H.Shinaoka, T. Someya. T. Sakurai, S. Takagi, Appl. Phys. Lett. 86, 073511, 2005.

[8] [8] L. Torsi, A. Dodabalapur, Anal. Chem. 77,380, 2005.

[9] Mabeck T.J., Malliaras G.G. Anal Bioanal Chem **384**: 343, 2006.

[10] [10] I. Manunza, A. Sulis, A. Bonfiglio, Appl. Phys. Lett. 89, 143502, 2006.

[11] [11] A. Bonfiglio, F. Mameli, O. Sanna, Appl. Phys. Lett. 82, 3550, 2003.

Inkjet printed arrays of pressure sensors based on all-organic field effect transistors

Laura Basiricò1, 2, Piero Cosseddu1, 2, Annalisa Bonfiglio1, 2, Rohan Neelgund, Harry W. Tyrer, member IEEE

Abstract— **In this paper we propose totally flexible organic field effect transistors (OFETs) assembled on plastic films as sensors for mechanical variables. First mechanical sensors for pressure and bending detection are presented. A sharp and reversible sensitivity of the output current of the device to an elastic deformation induced by means of a mechanical stimulus on the device channel has been observed and suggested the idea of employing arrays of such sensors for detecting the deformation applied onto a planar surface. Second the possibility of using similar devices for bio- and chemo-detection is described. By exploiting the properties of the basic structure, the device can be combined with any kind of substrate to detect for instance the pressure applied by people walking or standing on a functionalized carpet. This emerging technology seems to be promising for applications in the field of remote and non invasive monitoring of elderly and disabled people.**

I. Introduction

The light weight, low-cost processing, and the mechanical flexibility of conjugated polymers are a valuable alternative to most common inorganic materials for the realization of electronic devices. OFETs are recognized as key tools/building blocks for the implementation of electronic logic circuits [1, 2] and have been intensively studied for many applications, such as displays, smart tags and sensors [3]. Despite the low mobility of organic materials (compared to crystalline semiconductors, it is about three orders of magnitude lower) there are applications, as the recently suggested electronic skin [4], in which the lower speed is tolerable and the use of organic materials seems to be more beneficial than detrimental. In fact, being able to obtain large sensing areas is certainly a benefit for a wide set of applications and using low cost fabrication techniques could certainly widen the set of possible applications where sensing is required. OFET based mechanical sensors are active devices: many[1] different electronic parameters not only one, as for instance in piezoresistive sensors, can be extracted from their electrical characterization. Therefore, they are multiparametric sensors, offering the possibility of using a combination of variables in order to characterize their response to the parameter to be sensed. Finally, active sensors combine in the same device both switching and sensing functions; which easily allows applications for sensing a matrix of limited size and improved reliability. However, only a few examples of mechanical sensors have been reported so far [5, 6].

Mechanical flexibility is one of the main advantages of organic materials, yet organic semiconductor's strain properties have not been fully exploited in order to realize devices for detecting physical parameters as for instance pressure or bending.

The effect of strain on the mechanical and electronic properties of organic semiconductors is an emerging research topic in fundamental physics and applications. In this paper, we report on the realization of arrays of organic field-effect transistors that have been employed for pressure detection on relatively large surfaces.

II. Experimental

We recently proposed an innovative, organic field-effect transistor structure based on pentacene for pressure and strain detection [7, 8]. As can be easily seen from Figure 1, where a cross section of the structure is shown, OFETS based mechanical sensors gave rise a marked sensitivity of the drain current to an elastic deformation induced by mechanical stimulus on the device channel.

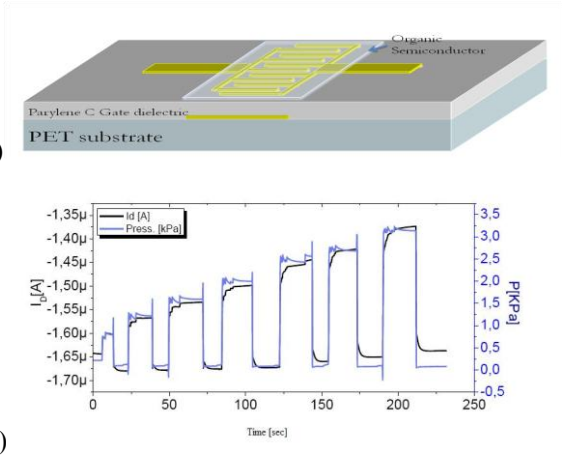

Fig. 1. Cross section of OFET based pressure sensor (a) and its electrical response to an external mechanical stimulus (b).

Applying a certain mechanical stress to the organic active layer induces a reversible change in its conductivity, which in turns led to a reversible change in the device output current (see Fig. 1b). A careful analysis of the

[1] Manuscript received May 27, 2010. Laura Basiricò, Piero Cosseddu, and Annalisa Bonfiglio are with the Department of Electrical and Electronic Engineering, University of Cagliari, Piazza d'Armi, 09123 Cagliari, Italy S3 nanoStructures and bioSystems at Surfaces, CNR-INFM, via Campi 213A, I-41100 Modena, Italy
Rohan Neelgund and Harry W. Tyrer are with the Department of Electrical and Computer Engineering , University of Missouri – Columbia, Columbia Missouri 65211, Dr. Tyrer is the corresponding author, phone 573 882 6489, and email tyrerh@missouri.edu

pressure dependence of the current also showed that this dependence can be explained in terms of variation in the mobility, in the threshold voltage and in the contact resistance of the transistor, and is correlated to the morphological and structural changes taking place within the organic semiconductor upon mechanical stimulus application [8].

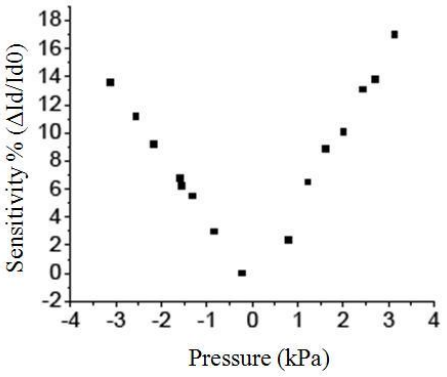

Fig. 2 Sensitivity vs applied pressure. Pressure was applied on both sides of the structure in order to achieve elongation (positive values) and compression (negative values) of the active layer.

Very interestingly, it can be also noticed that, for applied pressures ranging from -10 to +10kPa, the drain current variation upon deformation is linear and reproducible. The typical sensor response to the applied mechanical stimulus ranges from tens to hundreds of milliseconds, even though the time required to reach a steady state is usually in the range of tens of seconds, and the devices are able to detect pressure variations in the order of 0.1 kPa, with a measured sensitivity $(\Delta I/I_0)/(\varepsilon)$, where $\Delta I/I_0$ is the relative variation of drain current upon mechanical stimulus and ε is the strain, close to 5000.

The main peculiarity of this structure is that it is assembled starting from a highly flexible insulating film. Thanks to this feature, both sides of the insulating layer are accessible so it is possible to apply to both of them an external stimulus (i.e. a pressure) or to glue the final flexible device onto whatever kind of substrate (for instance a 3-D surface). This is usually impossible for structures assembled on a rigid substrate as, typically, OFETs realized on Silicon/Silicon dioxide, in which the presence of the substrate drastically limits the flexibility of the device.

In order to fully exploit organic electronics capabilities, the development and employment of easy, low temperature and low cost technologies for device fabrication is highly required. Among several, ink jet printing of polymers is surely the most promising and interesting. In contrast, subtractive processes is formed by depositing a homogeneous layer of material by spin coating over all the substrate and the final pattern is achieved subtracting excess material. However we use drop on demand ink jet printing, which is based on an additive process i.e. only material of interest (few picoliters) is deposited. Another huge advantage is that, as ink jet printing is a non-contact technique, substrate is in contact only with materials that made up the device and this lowers damage and contamination risk.

All organic FETs have been fabricated using a bottom-gate/bottom-contact structure (see Fig. 3) on a 175µm thick transparent and flexible polyethylene terephthalate sheet (PET, Goodfellow). The substrate was cleaned by ultrasonication in subsequent acetone and isopropyl alcohol baths, washed in de-ionized water and drying under nitrogen flow. Gate, source and drain bottom-contact were fabricated in air on a Fujifilm Dimatix 2800 drop on demand inkjet printer with a DMC-11610 cartridge. The cartridge contains 16 nozzles with a diameter of 21.5µm, each nozzle generates 10pL drops. For all electrodes we use a waterborne dispersion of the conducting polymer complex poly(3,4-ethylene-dioxy-thiophene) doped with polystyrene sulfonic acid (PEDOT:PSS Clevios P from H.C.Starck), the most employed conductive polymer in Organic Electronics. The dispersion is made of sub-micrometer sized gel particles, which after solvent drying and thermal annealing, form a continuous and transparent conductive film. Before filling the cartridge, solution has been filtered with a 0.45µm nylon filter in order to avoid nozzle clogging. During printing PEDOT:PSS based ink was at a constant temperature of 30°C and the PET substrate at 60°C to promote fast solvent drying, and to reduce ink spreading on the substrate. First, two layer gate electrodes were printed on the PET substrate. After printing, samples were let drying in an oven at 40°C for 12h. After that a thin 1.5µm Parylene C film, used as gate dielectric, was thermally sublimated on the structure.

PEDOT:PSS source and drain electrodes were then inkjet printed on the Parylene surface using a 5 µm drop spacing in an interdigitated configuration. The channel length (L) and width (W) realized were 150µm and 4.5cm respectively. We have realized a matrix of 7 interdigitated OTFTs into a 3cm equilateral triangular PET substrate using a common source configuration. Devices have been placed into two different rows, as shown in Fig. 3, each row with a common gate. All the assembled devices have independent drain electrodes in this way all the devices within the same matrix can be independently biased and measured.

Finally, in order to obtain the final device, an organic semiconductor thin film has been deposited. We have employed two different organic semiconductors and different deposition techniques for the active layer, to compare devices' performances different materials and deposition methods. A 50nm thick Pentacene (Sigma-Aldrich) film was vacuum sublimated on the channel region, while a poly(3-hexylthiophene)

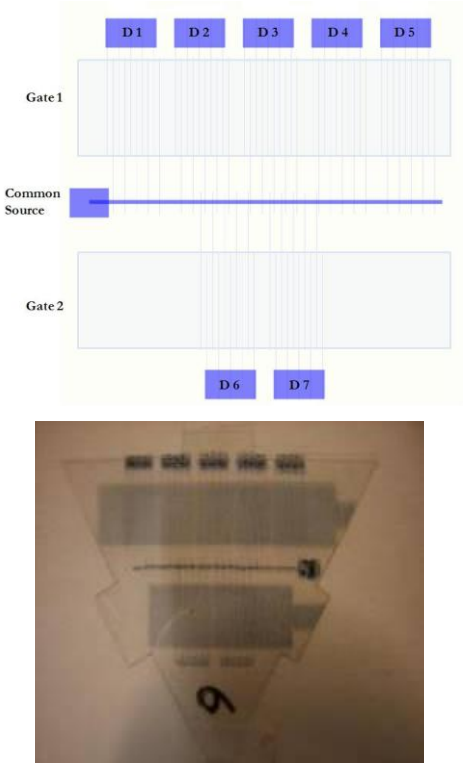

Fig. 3. Printed OTFTs matrix layout (a); top view of the real printed devices (b)

(P3HT) (Rieke Metal) based solution was deposited both both by inkjet printing and spin coating. The P3HT-based ink was filtered with a 0.2µm filter and kept at 40°C while substrate at room temperature during printing process. After deposition samples with P3HT as semiconductor were annealed at 130°C for 1h in hot plate.

III. Results

As can be clearly seen from Fig. 4(a) all organic devices realized using pentacene as active organic layer gave rise to the typical unipolar p-type behaviour, with charge carrier mobility up to $7x10^{-2}cm^2/Vs$ and Ion/Ioff ranging around 10^5. Very interestingly, no significant differences in the electrical behaviour have been noticed for all devices within the same matrix, meaning that this approach is highly reproducible.

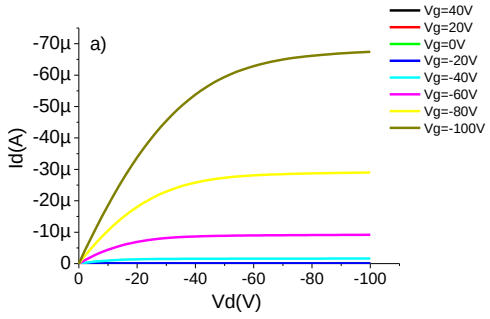

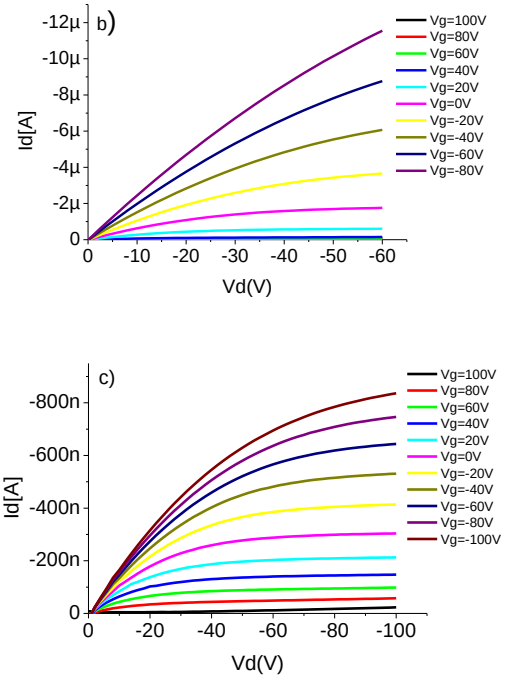

Fig. 4. Output characteristics of inkjet printed TFTs with PEDOT:PSS electrodes realized with different organic semiconductors: thermal evaporated pentacene (a); spin coated P3HT (b); inkjet printed P3HT (c)

As expected, using P3HT as organic semiconductor led to a significant decrease in charge carrier mobility, nevertheless all the devices realized by means of spin coating showed nice electrical behaviour with slightly lower mobility than the previously reported ones. In fact, even though P3HT is certainly one of the best performing solution processable polymers in terms of charge carriers mobility, it is well known from the literature that its average mobility is almost one order of magnitude lower than pentacene based OTFTs [9]. Considering the electrical behavior of inkjet printed P3HT devices, reported in Fig. 3 (c), despite a clear field effect behavior can be noticed, these devices are characterized by a much lower charge carrier mobility. The main reason for this behavior is to ascribe to much poorer quality of the active layer deposited by inkjet printing, which is strongly correlated to the final deposited film morphology. This can be improved either by a proper optimization of the polymeric ink and/or by an accurate optimization of deposition parameters.

IV. Applications: A Smart Carpet for Remote Monitoring

An important application is to use area detectors to monitor the elderly. Falls are a leading cause of death of the elderly. Detecting the walking pressure or the individual prone on the floor can provide a rapid means

to alert care givers to respond to falls. This can also provide security. In security the area sensor detects personnel in unexpected locations.

In operation, the sensor signal is amplified then forwarded to a microprocessor and to a computer. Determining which sensors send the data can be performed either by polling or by interrupt. From the microprocessor and the computer much intelligence can be provided, but initially they will provide display to a map of the floor. The variables that allow for choice of sensor architecture include the power supply, the geometric arrangement of the arrays and the signal detection matrix. For example one configuration is to set the power supply lines fixed and to obtain row and column data from FET source. Such an arrangement avoids the mxn detection and allows for m+n data lines. An important issue is the low level of sensor current that must be amplified; furthermore the high impedances allow for low currents.

Finally future work will be to test these in a practical setting. We have created a mock up floor to determine the best placement of sensor and carpet, and to determine that there is no slippage or cushioning. Individuals with dementia expend significantly more effort in walking than those with out cognitive challenges.

V. Conclusions

In conclusion, we have introduced a novel system suitable for the realization of mechanical sensors, based on organic thin film transistors. We demonstrated that these devices can be realized by means of very easy, reproducible over large area and cost efficient techniques, such as inkjet printing, opening the way for a wide range of applications. These results are very promising in view of innovative applications in the field of remote and non invasive monitoring of elderly and disabled people. Moreover, thanks to the high flexibility of the final structure, this approach can be employed for the fabrication of innovative electronics such as sensorized smart clothes for physiological parameter detection, or even in robotics for the realization of artificial "robot skin".

Acknowledgments

The American Alzheimer Association is gratefully acknowledged for funding the project under the ETAC Program.

The European Commission is gratefully acknowledged for funding the project under the Programme IST-ICT, VII FP Project n. 231500, ROBOSKIN

P.C. aknowledges Regione Autonoma della Sardegna (RAS) for funding his research under the PO Sardegna FSE 2007-2013, L.R.7/2007 "Promozione della ricerca scientifica e dell'innovazione tecnologica in Sardegna"

References

[1] C. D. Dimitrakopoulos, P. R. L. Malenfant, "Organic Thin Film Transistors for Large Area Electronics" Adv. Mater. vol. 14**,** nr. 2, p. 99-117, 2002

[2] B. Crone, A. Dodabalapur, Y.-Y. Lin, R. W. Filas, Z. Bao, R. Sarpeshkar, H. E. Katz, W. Li, "Large-scale complementary integrated circuits based on organic transistors" Nature vol. 03, p. 521-523, 2000

[3] T. Someya, T. Sekitani, S. Iba, Y. Kato, H. Kawaguchi, T. Sakurai, "A large-area, flexible pressure sensor matrix with organic field-effect transistors for artificial skin applications" PNAS vol. 101, nr. 27, p. 9966-9970, 2004

[4] T. Someya, Y. Kato, T. Sekitani, S. Iba, Y. Noguchi, Y. Murase, H. Kawaguchi, T. Sakurai, "Conformable, flexible, large-area networks of pressure and thermal sensors with organic transistor active matrixes" PNAS vol. 102, nr. 35, p. 12321-12325, 2005

[5] H. Kawaguchi, T. Someya, T. Sekitani, T. Sakurai, "Cut-and-Paste Customization of Organic FET Integrated Circuit and Its Application to Electronic Artificial Skin" IEEE J. Solid State Circuits vol. 40, nr. 1, p. 177–185, 2005.

[6] G. Darlinski, U. Böttger, R. Waser, H. Klauk, M. Halik, U. Zschieschang, G. Schmidt, C. Dehm, "Mechanical force sensors using organic thin-film transistors" J. Appl. Phys. Vol. 97, p. 93708, 2005.

[7] I. Manunza, A. Sulis, A. Bonfiglio, Appl. Phys. Lett. 89, 143502, 2006

[8] I. Manunza, A. Sulis, A. Bonfiglio, "Pressure and strain sensing using a completely flexible organic transistor", Biosensors & Bioelectronics, vol. 22: 2775-2779, 2007

[9] S. K. Park, Y. H. Kim, J. I. Han, D. G. Moon, W. K. Kim, M. G. Kwak "Electrical characteristics of poly (3-hexylthiophene) thin film transistors printed and spin-coated on plastic substrates", Synthetic Metals 139, p. 377–384, 2003

Faux-Floor Development System for Personnel Detection Using Signal Scavenging Sensors

Harry W. Tyrer, PhD, member, *IEEE,* Rohan Neelgund, Uday Shriniwar, Krishna Kishor Devarakonda, member*, IEEE*

***Abstract*—Motivated by the need to detect motion in elderly people, resulting in falls, we have developed a low cost sensor system using aluminum foil as the sensor of static electricity and electromagnetic energy. But to make this a system we need to amplify the data and use it by displaying the motion or activity of a person. We constructed a faux floor development board to provide an initial pilot test of the idea of using stray electric energy, or as we call it signal scavenging. The foils are placed on the faux floor (in this case a 1 m X 1 m wooden surface) allowing foil excitation from the motion of a test subject. The faux floor is a useful tool allowing testing of different foils, analog and digital electronics circuits and different carpeting. Importantly, even though the system supported a small number of foil sensors its performance characteristics clearly show the excellent detection capability of the system. Testing the timing characteristics resulted in reading the 4 sensors in 3.11 msec, indicating that for even a large system of a few hundred sensors we can poll the foils in sufficient time to detect the motion of people. Our data show true positive rates of 98% and false positive and false negative rates of 2%, a high detection rate. Using the development board has provided much helpful information on the use of signal scavenging for personnel detection.**

I. INTRODUCTION

WITH the aging of the population around the world [1, 2, 3 ,4], there is increasing concern of the severity of falls and the associated effect on the elderly. For example improper medicine dose may lead to a fall which may lead to depression then loss of appetite and death, and approximately 15% of deaths are dues to falls of the elderly [5, 6, 7]. The objective then of providing elder technology should be first to improve the quality of life, that is allow for longer life as the individual declines. A second objective is to provide longer independent living in a safe comfortable environment. Finally to provide care givers and loved ones with additional resources and support that reduces cost and improves their ability to provide care.

Manuscript received May 27, 2010. Harry W. Tyrer, PhD, Rohan Neelgund, Uday Shriniwar, and Krishna Kishor Devorakonde, are with the Department of Electrical and Computer Engineering , University of Missouri – Columbia, Columbia Missouri 65211, Dr. Tyrer is the corresponding author phone 573 882 6489, and email tyrerh@missouri.edu

While there is much technology available for the elderly [3, 4], we have focused primarily on monitoring devices and communicating the monitored results to the caregivers and loved ones.

We have constructed a development board faux floor that we use to build and test devices. The purpose of this floor is to guide our development of a full floor for personnel detection. The faux-floor must be able to provide a means of testing the sensors and electronics for initial development. It needs to support the weight of individuals performing the tests, be sufficiently rugged to withstand motion and assess limited dynamic interactions, and to demonstrate the working of the sensors and electronic in a setting similar to that which would be expected in the normal course of operation. In this paper we are able to assess the performance of our static personnel sensor using ROC curves.

II. THE DEVICE AND MEASUREMENTS

Our sensors are rectangular aluminum foil sheets connected to an electronics board then connected to a display. Through some effort we developed a signal scavenging technique to detect the presence of a person on a floor. Basically we are detecting both static and stray electricity, and we have characterized some of the properties of this energy. The electro-magnetic component consists primarily of stray 60 cycle energy with the fundamental by far the most prominent component and we are able to distinguish up to the 10^{th} component. We regularly see both even and odd Fourier components [8]. The detection is due to increased energy into the foils due to a person on or near the foils. An interesting and promising characteristic is that we see a monotonically increasing response with size, while maintaining the separation between activated (that is touched) foils and non-activated.

Figure 1: Development board carpet is atop a wooden frame (made up of 5cm X 10 cm, i.e. 2 X 4 studs) approximately 1 m X 1 m. The four sensors are under the carpet; wires come through the wooden frame and attach to the circuit board shown

We constructed a faux floor to support the sensors by placing a 1 m X 1 m X 16 mm (3 ft sq ¾ inches) thick piece of plywood board on a square frame of 5 cm X 10 cm (2" X 4") wood studs. A suitable stud provided additional support at the center. On to this we placed the sensors separated with

a plastic foil; this was all then covered with an institutional carpet. We placed 4 foils on this system and identified the approximate position of the foils under the carpet. Figure 1 show the completed faux floor development board. The figure shows the carpet over the array of four sensors; the sensors do not require external power supply or batteries.

However the supporting electronics do require power. The foil connects to a high impedance amplifier which detects the signal energy. Overall the signals are then converted to digital signals, and formatted for display on a PC screen as shown in figure 2.

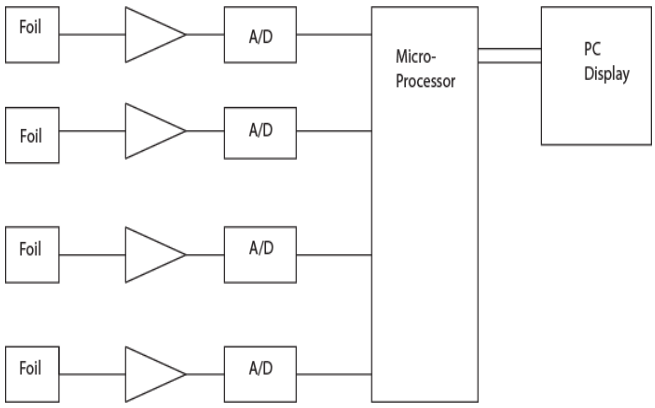

Figure 2: Foil reading electronics. Foil voltage is amplified, and formed into a pulse, effectively converting it to a digital value. The microprocessor polls the it's four ports for the pulse signals producing a formatted serial data stream sent to the computer.

Nevertheless there is much complication required by the overall problem and the circuit reflects that. The amplifier is not a straight forward linear device. We are after all detecting noise and substantial effort went into generating a relatively square signal of 5 volts at the output.

We are detecting not only the 60 Hz stray electromagnetic ubiquitous noise, but we are also detecting a pulse signal due to static charge and discharge; as activation takes place the activator discharges into the conductor and as deactivation occurs the conductor returns to its original charge configuration. This produces an additive signal that enhances the properly prepared 60Hz component. The result is a reasonably well behaved and predictable pulse that can be detected.

Consequently in the implementation of the electronic system we did not actually place A/D converters, but went directly into the microprocessor. This is an important characteristic because of the need to make the circuit board unobtrusive (say in a home setting) large numbers of independent A/D converters would work against that possibility. So for this implementation we chose to consider only pulse detection and no intermediate values.

Since we expect our final implementation to include several hundred and even thousands of foils it will be prohibitive to provide a standalone amplifier and A/D converter, nevertheless a possible implementation will be to use an A/D converter that will deal with noise and signal noise. (That is the modulation of the noise by the activation of the foil. This will provide and interesting and important alternative.

The microprocessor provides an interface to a computer to provide display. Polls the input ports to read the pulse, places the active foil name (A, B, C, D) into a character stream and outputs the data at 19,200 Baud. Our timing data shows that this occurs in less than one millisecond, so that for our purposes this is sufficient (data not shown). The serial data then enters the computer where we displayed it in a format that reflect the sensor arrangement on the board (Figure 3, below). Since the development floor is a laboratory device, the best display arrangement for performance data acquisition was to divide the screen into 4 parts and display the activated quarter in a contrasting color, in this case the background was green and the activated quarter(s) in red. Figure 3 shows the display in action: The upper figure shows the person standing on the carpet activating foil C, the display shows red in the lower left quadrant, which corresponds to C. Similarly the lower figure showed the activation of foils A and B and the display shows the corresponding quadrants in red indicating activation.

Figure 3: Person standing on the carpet activating sensor C (upper) and both sensors A and B (lower). The green background LCD displays the activated sensor in red. Note the red screen quartile in the lower left quarter of the display of the upper figure. Similarly the activation of A and B causes the lower half of the screen to turn red.

III. RESULTS

We have previously described the operation of the individual foils, have tested the individual components and noted their performance [8]. Here, we have reviewed the operation of the foils, will describe the interactions of the system, the

microprocessor data formatting, and provide an assessment of the detection capability of the system.

We have tested the microprocessor both for data accuracy and time of operation. First consider the data. We have looked at the formatted data in list mode in the display computer. The data transfer for say foil A and B activation (Fig 3 lower) has the following appearance: **S12E,** S for Start and E for End, and the number corresponds to the alphabetic designation of the foil: A is 1 … D is 4. Figure 4 is a cut of the list mode data showing the excitation of all 4 sensors. The first 6 characters show the data train (S1234E).

We tested all possible combinations of A, B, C, and D, and obtained similar results. Furthermore we visually correlated the activation with the data train and the display and observed consistent results.

S1234E15541S1234E15541S1234E15541S1234E15
34E15541S1234E15541S1234E15541S1234E15541
15541S1234E15541S1234E15541S1234E15541S12
41S1234E15541S1234E15541S1234E15541S1234E

Figure 4: The raw formatted data sent to the computer by the microprocessor. In this case S1234E indicates the stream start followed by excitation of the A, B, C, D and the end of the data stream. This repeats after the count of the number of clock pulses required to poll the microprocessor ports.

Now the time for polling is also shown in Fig 4 following the data transfer, and is the number of timer pulses required to obtain that data (e.g. 15541). We excited foils and counted the number of clock cycles for each poll of the data set. We then converted the number of pulses to time using the 4 MHz clock and obtained the time required to read foils. We did this for 1, 2, 3, and 4 foils. The result is that increasing the number of foils activated increases the polling time.

No. of Active Sensors	Time in Milliseconds
0	1.03
1	1.43
2	2.07
3	2.59
4	3.11

Table 1: Time required polling the data ports of the microprocessor

Table 1 shows the set of experiments carried out at 19,200; we also carried the data out at other transmission channel rates. Since the data shows similar (but smaller) time characteristics we do not show the data. Note that the base line (no active sensors) poll time is 1 msec or so, so that one sensor only requires 0.43 msec longer. With a second sensor the time should double after removing the base value, but the data shows that is increased 2.43 times. Each such increase produces an increased time more than an integer number of sensors but nevertheless proportional to the number of sensors.

A more comprehensive evaluation is to excite the individual foils and count the number of true positives, the number of false positives (display of positive to a non-activated foil), and false negatives (non-display of activated foils). We gathered the data by manually activating a foil 50 times at a rate approximately one step per second and visually note the display. Table 2 shows the development board detection performance. Since each sensor was activated 50 times, the numbers in the diagonal cell indicates the number of times that the sensor did not cause the display to turn red,

50	A	B	C	D
A	1	1	0	0
B	0	4	0	2
C	0	0	4	0
D	0	0	0	3

Table 2: Columns show the activated sensors, row shows the display readings. Diagonal show the numbers of non responses when foil activated. Off diagonal terms indicate response when another sensor is activated.

that is, the false negatives; so calculate the true positives by subtracting the numbers in the diagonal cells from 50. Similarly the off diagonal terms contain the number of times that activating a foil caused another sensor on the board to display as positive, that is false positives.

We show false positives as activating the sensor in the row causing a column sensor to display positive. For example stepping on A 50 times caused B to illuminate once for a total true positive of 49.

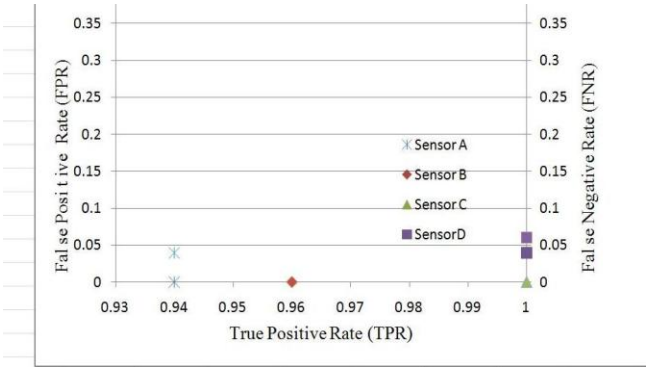

Figure 5: Summarizing the result of 50 steps (activations) on each sensor. Left ordinate indicates false positives, right ordinate indicates false negatives, abscissa shows true positive.

A representation in ROC space helps to appreciate the high degree of accuracy that this system, provides in detecting foil activity. Figure 4 shows both false positive and negative rates which correspond to the same true positive rate.

In point of fact it turned out to correspond to the same foil. First note that the false positive and negative data is all less than 5% and that most of it is at or near zero, second note that we the true positive rate is 94% and higher. This and other experience increases our confidence that the system will be useful using signal scavenging to detect personnel motion.

IV. DISCUSSION

We designed and constructed a faux floor development to have an easily accessible and changeable means of trying out our ideas in the development of a personnel sensing system. This has been a very useful way to test each individual part of the system from the foil and its' attachment to wires to the display.

It was important to set up a system that is known to work then make the changes and observe improvements. The development board provides the capability to make changes in the electronic system and identify the best way to proceed. We have found the appropriate characteristics of the amplifier to allow us to set up the floor in different environment. It is useful to repeat that we are detecting noise and there is considerable influence of the environment on the noise data that we acquire. Similarly we were able to test several microprocessors systems and data acquisition systems. Furthermore it was very useful in providing the heuristic experience necessary to gain confide in the operation of the devices.

Perhaps most important is the performance data that we have generated as shown in this paper and as we have operated the development board. The high degree fidelity for the data, with low error rates provides encouragement that the approach is correct and will yield useful results. Furthermore we have identified sources of error in the construction of the faux floor development system that contributes to the errors shown here in the performance data. The performance data led us to observe a slight misalignment due to the drying of the wood that caused small but in some cases detectable errors on the other foils.

Ongoing work on the prototype continues; for example, to identify the optimal impedance for circuits leading from the sensors, refine the resolution of signals, and develop programming to send messages to alert caregivers. And early results are encouraging for detecting falls.

V. CONCLUSIONS

We have constructed and tested a faux floor development board. The board provides us with a means to arrange foils on flat surface, activate the foils, and connect to the electronics sub-system which can be interchanged. We have used this feature to develop and optimize our electronics and data transfer resources.

More importantly this gives a useful demonstration that the pulse detection of stray electromagnetic energy properly combined with static charge and discharge provides a useful means of personnel detection using signal scavenging.

ACKNOWLEDGEMENTS

We gratefully acknowledge The Alzheimer Association for funding the project under the ETAC Program. Jim Fischer and Marty Walker contributed greatly to this project. We gratefully acknowledge his support.

REFERENCES

[1] Tyrer, H., Alwan, M., Demiris, G., He, Z., Keller, J., Skubic, M., Rantz, M., "Technology for Successful Aging", *Proceedings, IEEE 2006 International Conference of the Engineering in Medicine and Biology Society*, New York, NY, August 30-September 3, 2006, pp. 3290-3293.

[2] Demiris, G., Rantz, M.J., Aud, M.A., Marek, K.D., Tyrer, H.W., Skubic, M., & Hussam,A.A. (2004). Older adults' attitudes towards and perceptions of "smart house" technologies. *Medical Informatics and the Internet in Medicine, 29(2), 87-94.*

[3] Rantz MJ, Porter R, Cheshier D, Otto D, Servey CH, Johnson RA, Skubic M, **Tyrer H**, He Z, Demiris G, Lee J, Alexander G, & Taylor G TigerPlace, a State-Academic-Private Project to Revolutionize Traditional Long Term Care, *Journal of Housing for the Elderly*, *22*(1/2), 66-85, 2008

[4] **Tyrer HW**, Aud MA, Alexander G, Skubic M, Rantz M. Early Detection of Health Changes in Older Adults, *Proc., IEEE 2007 Intl. Conf. of the Engineering in Medicine and Biology Society*, Lyon, France August, 2007, pp. 4045-4048.

[5] Tinetti ME, Speechley M, Ginter SF. Risk factors for falls among elderly persons living in the community. *N Engl J Med*. 1988;319:1701–1707

[6] Van Dijk PT, Meulenberg OG, van de Sande HJ, et al. Falls in dementia patients. *Gerontologist*. 1993;33:200–204

[7] Liu-Ambrose T, Ashe, M.C, Graf P, Beattie, B.L. and Khan, K.M. Increased Risk of Falling in Older Community-Dwelling Women With Mild Cognitive Impairment Phys Ther Vol. 88, No. 12,1482-1491,2008

[8] Harry W. Tyrer, Rohan Neelgund, Ashrafuddin Mohammed, Uday Shriniwar Signal Scavenging For Passive Monitoring In Eldercare Technology, Proceedings of the 31st Annual International Conference of the IEEE EMBS (paper number 15901410), Minneapolis, Minnesota, USA, September 2-6, 2009, pages 6167 – 6170